Development 130, 2513-2524

doi:10.1242/dev.00459

DEVELOPMENT AND DISEASE

Role for growth factors and extracellular matrix in controlling differentiation of prospectively isolated hepatic stem cells

Atsushi Suzuki[1], Atsushi Iwama[2], Hitoshi Miyashita[1], Hiromitsu Nakauchi[2] and Hideki Taniguchi[3,*]

[1]Department of Surgery, Institute of Clinical Medicine, University of Tsukuba, Tsukuba, Ibaraki 305-8575, Japan
[2]Laboratory of Stem Cell Therapy, Center for Experimental Medicine, Institute of Medical Science, University of Tokyo, Tokyo 108-8639, Japan
[3]Department of Regenerative Medicine, Faculty of Medicine, Yokohama City University, Yokohama, Kanagawa 236-0004, Japan
*Author for correspondence (e-mail: rtanigu@med.yokohama-cu.ac.jp)

Accepted 26 February 2003

SUMMARY

In liver development, a number of growth factors (GFs) and components of the extracellular matrix (ECMs) lead to differentiation of liver parenchymal cells. As the liver contains many cell types, specifically investigating their functional effects on hepatic stem cell populations is difficult. Prospective isolation and clonal assays for hepatic stem cells enable the examination of direct effects of GFs and ECMs on this rare cell fraction. Using previously purified cells that fulfill the criteria for hepatic stem cells, we examined how GFs and ECMs regulate differentiation in the developing liver. We show here that hepatocyte growth factor (HGF) induced early transition of albumin (ALB)-negative stem cells to ALB-positive hepatic precursors resembling hepatoblasts and then oncostatin M (OSM) promoted their differentiation to tryptophan-2, 3-dioxygenase (TO)-positive mature hepatocytes. During this transition, ECMs were necessary for the differentiation of stem cells and precursors, but their effects were only supportive. In the first step of stem cell differentiation induced by HGF, the expression of CCAAT/enhancer binding protein (C/EBP), a basic leucine zipper transcription factor, changed dramatically. When C/EBP function was inhibited in stem cells, they stopped differentiating to hepatocyte-lineage cells and proliferated actively. These are the first findings to illustrate the mechanism of hepatic stem cell differentiation in liver development.

Key words: Stem cell, Liver, Hepatocyte, C/EBP, Mouse

INTRODUCTION

In mouse embryogenesis, the liver primordium initially develops from the ventral foregut endoderm at embryonic day (E) 8 (Wilson et al., 1963; Zaret, 2000). Signals from the adjacent cardiac mesoderm and septum transversum, which are mainly mediated by fibroblast growth factors (FGFs) and bone morphogenetic proteins (BMPs), induce cells to express albumin (ALB) and α-fetoprotein (AFP), and to initiate liver bud formation (Jung et al., 1999; Rossi et al., 2001). After the specification of the liver, hematopoietic cells move into this organ and produce oncostatin M (OSM), which induces the maturation of hepatocytes (Kamiya et al., 1999; Kinoshita et al., 1999). At postnatal stages, hepatocyte growth factor (HGF) produced by non-parenchymal liver cells (sinusoidal, stellate and endothelial cells) is involved in hepatic maturation (Hu et al., 1993; Kamiya et al., 2001). These findings demonstrate that several signals mediated by mesoderm-derived cells steer cell fates towards hepatic lineages and induce differentiation into functional hepatocytes. It is not known, however, whether these signals act directly or indirectly to affect hepatic stem cell growth and differentiation. Thus, it is essential to examine the effects of such growth factors (GFs) in single-cell-based studies using purified stem cell populations.

In a previous study, using flow cytometry and single-cell-based assays, we prospectively identified hepatic stem cells with multilineage differentiation potential and self-renewing capability (Suzuki et al., 2002). These cells expressed the hepatocyte growth factor receptor Met and were low-positive for CD49f (α6 integrin subunit), but did not express Kit (stem cell factor receptor), CD45 (leukocyte common antigen) and TER119 (a molecule resembling glycophorin, exclusively expressed on immature erythroid cells). Sorted stem cells could be clonally propagated in culture for over 6 months, where they continuously produced hepatocytes and cholangiocytes as descendants, while maintaining primitive stem cells that expressed neither albumin nor cytokeratin 19 during the greater part of their expansion. Our studies with highly enriched populations with stem cell activity showed that HGF was a critical requirement

for proliferation (Suzuki et al., 2000; Suzuki et al., 2002). It remained unknown, however, whether the Met/HGF interaction had a role in stem cell differentiation. Spagnoli et al. (Spagnoli et al., 1998) established a bi-potential hepatic precursor cell line from transgenic animals that constitutively expressed the activated form of Met. This and our previous findings suggest that, while the Met/HGF interaction is crucially responsible for maturation of differentiating hepatocytes in the postnatal liver (Hu et al., 1993; Kamiya et al., 2001) and division of mature hepatocytes in liver regeneration (Michalopoulos et al., 1984; Ishiki et al., 1992), it is also involved, through a separate mechanism, in stem cell growth and differentiation.

In this study, we investigated the direct effects of GFs and extracellular matrix components (ECMs) on proliferation and bi-potential differentiation of prospectively isolated and clonally cultured hepatic stem cells. To analyze primitive stem cells and stem cell-derived differentiating hepatocytes, respectively, cell type was determined by the expression of ALB enhancer/promoter-EGFP. We demonstrated that HGF, but not FGFs, induced early transition from ALB-negative (ALB^-) stem cells to ALB-positive (ALB^+) hepatic precursors through signaling via the CCAAT/enhancer-binding protein (C/EBP), a basic leucine zipper transcription factor. Subsequently, HGF was an effective mitogen for differentiating cells, while OSM inhibited their proliferation and induced their maturation, as assessed by expression of glucose-6-phosphatase (G6P) and tryptophan-2, 3-dioxygenase (TO). By contrast, these factors suppressed differentiation into cholangiocyte-lineage cells. Inactivation of C/EBPs, even in the presence of both HGF and OSM, strongly inhibited the differentiation of stem cells into hepatocyte-lineage cells and allowed cells to self-renew efficiently. Although several ECMs could also induce differentiation of stem cells by regulating C/EBPs, their effect was much weaker and may just work supportively for stem cell differentiation. Our present data show that gradual effects from HGF and OSM, mediated by the transcription factor C/EBP, lead stem cells to differentiate into hepatocytes rather than cholangiocytes through the efficient expansion of differentiating cells and permissive signals inducing the maturation of hepatocytes.

MATERIALS AND METHODS

Flow-cytometric sorting and culture of hepatic stem cells

Stem cell clones were prospectively isolated from C57BL/6 embryonic day (E) 13.5 fetal mice (CLEA, Tokyo, Japan) and were clonally cultured as described (Suzuki et al., 2002). After the initiation of culture, cells were maintained in culture by replating them every 7 days. Three clones were randomly selected and those cells were used for examination. For the GF test, we used HGF (generous gift from Dr T. Ishii, Mitsubishi Pharma Corp), OSM (Sigma, St Louis, MO), acidic FGF (aFGF) (Peprotech, London, UK), and basic FGF (bFGF) (Peprotech), and for the ECM test, we used non-coated dishes, and laminin-, type IV collagen-, type I collagen- and fibronectin-coated dishes (Becton Dickinson, San Jose, CA).

Isolation of total RNA

We prepared total RNA from test samples and, as RNA standards for real-time PCR, from fetal, neonatal and adult liver, using an RNeasy Mini Kit (QIAGEN, Tokyo, Japan) according to the manufacturer's instructions. Total RNA was diluted and used for quantitative analyses.

Semi-quantitative RT-PCR analysis

Sorted 1×10^5 cells were used to prepare total RNA. After various dilutions of template cDNA, we optimized their concentration for each primer. In these concentrations, amplification by PCR did not reach plateau but could be used semi-quantitative analysis. PCR was conducted using hepatocyte-specific primers for albumin (ALB), α-1-antitrypsin (αAT), glucose-6-phosphatase (G6P), and tryptophan-2,3-dioxygenase (TO), and for positive control hypoxanthine phosphoribosyltransferase (HPRT) as described (Suzuki et al., 2000; Suzuki et al., 2002). PCR cycles were as follows: initial denaturation at 95°C for 4 minutes followed by 40 cycles of 94°C for 1 minute, 56°C for 1 minute, 72°C for 1 minute and final extension at 72°C for 10 minutes. PCR products were separated in 2% agarose gel.

PCR primers and TaqMan fluorogenic probes

PCR primers and TaqMan fluorogenic probes for real-time quantitative PCR were designed using the Primer Express software program (Version 1.0) (Applied Biosystems, Tokyo, Japan). The sequences were as follows: hepatocyte-differentiation primers for ALB (forward, 5′-TGT CCC CAA AGA GTT TAA AGC TG-3′; reverse, 5′-TCT TAA TCT GCT TCT CCT TCT CTG G-3′; and probe, 5′-ACC TTC ACC TTC CAC TCT GAT ATC TGC ACA CT-3′), α-fetoprotein (AFP) (forward, 5′-CCT GTC AAC TCT GGT ATC AGC CA-3′; reverse, 5′-CTC AGA AAACTG GTG ATG CAT AGC-3′; and probe, 5′-TGC TGC AAC TCT TCG TAT TCC AAC AGG A-3′), αAT (forward, 5′-TCG GAG GCT GAC ATC CAC AA-3′; reverse, 5′-TCA ACT GCA GCT CAC TGT CTG G-3′; and probe, 5′-TTC CAA CAC CTC CTC CAA ACC CTC AA-3′), G6P (forward, 5′-GTT CAA CCT CGT CTT CAA GTG GAT-3′; reverse, 5′-TGC TGT AGT AGT CGG T GT CCA GGA-3′; and probe, 5′-TTT GGA CAA CGC CCG TAT TGG TGG-3′) and TO (forward, 5′-CAA GGT GAT AGC TCG GAT GCA-3′; reverse, 5′-TCC AGA ACC GAG AAC TGC TGT-3′; and probe, 5′-TGT GGT GGT CAT CTT CAA GCT CCT GG-3′); cholangiocyte-differentiation primers for cytokeratin 19 (CK19) (forward, 5′-TGA AGA TCC GCG ACT GGT-3′; reverse, 5′-TAA AGT AGT GGT TGT AAT CTC GGG A-3′; and probe, 5′-CCA GAA GCA GGG ACC CGG ACC-3′), and γ-glutamyltranspeptidase (GGT) (forward, 5′-TTT GCC TAT GCC AAG AGG AC-3′; reverse, 5′-TTG CGG ATC ACC TGA GAC A-3′; and probe, 5′-ATG CTC GGT GAC CCA AAG TTT GTC G-3′); or miscellaneous primers for hepatocyte nuclear factor 1 (HNF1) (forward, 5′-GCT AGG CTC CAA CCT TGT CAC G-3′; reverse, 5′-TTG TGC CGG AAG GCT TCC T-3′; and probe, 5′-AGG TGC GTG TCT ACA ACT GGT TTG CCA-3′), hepatocyte nuclear factor 4 (HNF4) (forward, 5′-TGG TGT TTA AGG ACG TGC TGC-3′; reverse, 5′-ACG GCT CAT CTC CGC TAG CT-3′; and probe, 5′-CAA TGA CTA CAT CGT CCC TCG GCA CTG T-3′), hepatocyte nuclear factor 6 (HNF6) (forward, 5′-CCG GAG TTC CAG CGC AT-3′; reverse, 5′-TCT TGC TCT TTC CGT TTG CA-3′; and probe, 5′-TCG GCG CTC CGC TTA GCA GC-3′), Met (forward, 5′-GAT CGT TCA ACC GGA TCA GAA-3′; reverse, 5′-GGA AGA GCC CGG ATA ATA ACA A-3′; and probe, 5′-TGC AGG ATT GAT CAT TGG TGC GGT C-3′), CCAAT-enhancer binding protein-alpha (C/EBPα) (forward, 5′-AGC AAC GAG TAC CGG GTA CG-3′; reverse, 5′-TTA TCT CGG CTC TTG CGC A-3′; and probe, 5′-CGG GAA CGC AAC AAC ATC GCG-3′) and CCAAT/enhancer binding protein-β (C/EBPβ) (forward, 5′-CGG ATC AAA CGT GGC TGA G-3′; reverse, 5′-CGC AGG AAC ATC TTT AAG GTG A-3′; and probe, 5′-ACG TGT AAC TGT CTA GCC GGG CCC TG-3′). All TaqMan probes used in this experiment carried a 5′ FAM reporter dye (Applied Biosystems).

Real-time PCR conditions

The RT and the PCR were performed in one step by using TaqMan EZ RT-PCR Core Reagents (Applied Biosystems). The reaction mixture (25 μl final volume) includes 100 or 500 ng total RNA.

5×TaqMan EZ buffer (5 μl), $Mn(OAc)_2$ (3 mM), rTth DNA polymerase (0.1 U/μl), uracil N-glycosylase (0.01 U/μl), dATP, dCTP, dGTP, dUTP (each 300 μM), and forward and reverse primers (200 nM), and probe (100 nM). Reverse transcription was performed at 60°C for 30 minutes. PCR was performed as follows: initial denaturation at 95°C for 5 minutes followed by 60 cycles of 95°C for 15 seconds and 60°C for 1 minutes. A template-free control was included in each experiment. All template-free controls, standard RNA dilutions and test samples were assayed in triplicate.

Analysis of real-time PCR data

The starting amount of mRNA in each test sample was calculated by preparing a standard curve using known dilutions of RNA standards. For each dilution, the ABI-PRISM 7700 software (Applied Biosystems) generated a real-time amplification curve constructed by relating the fluorescence signal intensity (ΔRn) to the cycle number. The ΔRn value corresponded to the variation in the reporter fluorescence intensity before and after PCR, normalized to the fluorescence of an internal passive reference present in the buffer solution. The standard curve was then generated on the basis of the linear relationship existing between the Ct value (cycle threshold: corresponding to the cycle number at which a significant increase in the fluorescence signal was first detected) and the logarithm of the starting quantity. Starting quantities of mRNA in samples were quantified by plotting the Ct on this standard curve.

Gene transfer into hepatic stem cell cultures

Stable transfection of hepatic stem cell cultures was carried out by lipofection. Briefly, 10 μg of a construct containing both the enhanced green fluorescence protein (EGFP) driven by the ALB promoter (–0.3 kb) and enhancer, a region located 8.5-10.4 kb upstream of the ALB promoter (Pinkert et al., 1987), and the Zeocin resistance gene was used to transfect 1×10^6 cells using Lipofectamine 2000 (Gibco BRL, Gaithersburg, MD). Stably transfected cells were selected by growth on laminin-coated dishes (Becton Dickinson) in our standard medium supplemented with 600 μg/ml Zeocin (Invitrogen, Groningen, Netherlands) and isolated by using cloning rings (Iwaki Glass, Tokyo, Japan). The frequency of EGFP-positive cells was assayed by FACS-Vantage (Becton Dickinson). In this paper, representative data from a transfected stem cell clone are shown because similar results were obtained from others.

Retrovirus production and FACS analysis of transduced cells

The retroviral vector pGCsam (MSCV) is described elsewhere (Kaneko et al., 2001). A dominant-negative form of C/EBP (A-C/EBP) followed by IRES EGFP or IRES nerve growth factor receptor truncated in the cytoplasmic domain (tNGFR) were subcloned into pGCsam (GCsam-A-C/EBP-IRES-EGFP, GCsam-A-C/EBP-IRES-NGFR, respectively). To produce recombinant retrovirus, plasmid DNA was transfected into 293gp cells (293 cells containing the *gag* and *pol* genes but lacking an envelope gene) along with 10A1 *env* expression plasmid (pCL-10A1) (Miller et al., 1996) by $CaPO_4$ co-precipitation, and supernatant from the transfected cells was collected to infect cells. To detect the expression of tNGFR on the cell surface, cells were stained by mouse anti-human NGFR (Chemicon, Temecula, CA) followed by phycoerythrin (PE)-conjugated rabbit anti-mouse Igs (Dako, Carpinteria, CA) and analyzed by FACS-Vantage (Becton Dickinson).

RESULTS

Purification of ALB⁻ and ALB⁺ cells from heterogeneous stem cell cultures

As an experimental source, we used fluorescence-activated cell sorting (FACS) to sort cells from the Met^+ $CD49f^{+\,low}$ Kit^- $CD45^-$ $TER119^-$ cell fraction in E13.5 fetal mouse livers, in which self-renewing multipotent hepatic stem cells are highly enriched, and then expanded these cells in clonal cultures. After cell transplantation of expanding stem cells, even into mice with immunodeficiency, we have never found abnormal development and tumor formation by donor-derived cells. Furthermore, karyotype-analysis using FACS and propidium iodide showed that they maintained normal G0/G1 (2n) and G2/M (4n) pattern similar to primary sorted cells. These results strongly suggest that those cells are not the product of transformation and are diploid without the karyotypic rearrangements.

To examine direct roles for GFs and ECMs in stem cell differentiation, stem cell clones were placed in several culture conditions and the state of differentiation was analyzed by using FACS and quantitative PCR (Fig. 1). In our stem cell cultures, however, in addition to self-renewing stem cells, differentiating progeny such as hepatocytes and cholangiocytes were spontaneously produced from stem cells. Owing to this heterogeneity, the target cells for the effects of GFs and ECMs could not be determined. To elucidate which steps of stem cell differentiation were affected by differentiation-inducible factors, we separated the original cell population into ALB^- and ALB^+ cells using FACS, following gene transfer of the ALB enhancer/promoter-EGFP construct into stem cell cultures (Fig. 1, Fig. 2A). After FACS-sorting, semi-quantitative RT-PCR analysis was conducted to compare the expression of hepatocyte markers in $EGFP^+$ (ALB^+) cells with that in $EGFP^-$ (ALB^-) cells. As expected, the expression of hepatocyte markers in ALB^+ cells was much higher than in ALB^- cells (Fig. 2B). These data clearly show that stem cell-derived differentiating heaptocyte-lineage cells can be visualized and specifically separated from other lineage cells. We next examined the expression of the liver-enriched transcription factors in ALB^- and ALB^+ cells. Interestingly, although there was little difference in the expression of HNF1 and HMF4 between ALB^- and ALB^+ cells in the result of real-time quantitative PCR analysis, the expression of HNF6, which is known to be a regulator of pancreatic endocrine cell differentiation (Jacquemin et al., 2000), was much higher in ALB^+ cells (Fig. 2C). These results suggest that HNF6 could be involved in hepatocyte-differentiation from hepatic stem cells in the liver development.

Following independent culture, both ALB^- and ALB^+ cells gave rise to ALB^+ as well as ALB^- cells as assessed by FACS and a confocal microscopy (Fig. 2A,D). In addition, those sorted ALB^- and ALB^+ cells capable of proliferation in culture, both possessed the capacity for differentiation into cholangiocytes (data not shown). These results demonstrated that ALB expression begins at a very early stage of stem cell differentiation, and that lineage specification into either hepatocytes or cholangiocytes cannot be determined by its expression. Therefore, early-differentiated ALB^+ cells may represent a bipotent hepatic precursor such as hepatoblasts, which express ALB and AFP, but are still capable of differentiating into cholangiocytes in the developing liver (Shiojiri et al., 1991).

Regulation of growth and differentiation of purified ALB^- and ALB^+ cells by GFs and ECMs

To examine the effects of GFs and ECMs on ALB^- and ALB^+

cells, sorted cells were independently cultured in six-well plates (1×10^4 cells/well) using several conditions and examined 10 days later. Although single cell cultures of sorted cells required ECMs and HGF similar to primary cultures, this high number of purified cells allowed slow growth even without GFs and ECMs. For ALB$^-$ sorted cells, HGF strongly induced their proliferation. FGFs had a smaller positive effect, while OSM, by contrast, inhibited their proliferation (Fig. 3A, upper left graph). For ALB$^+$ sorted cells, extensive proliferation was also found when cultured with HGF, but not with OSM and FGFs (Fig. 3A, lower left graph). The laminin, type IV collagen, and type I collagen were more effective on ALB$^+$ cells than ALB$^-$ cells (Fig. 3A, right graph). FACS analysis of cultured cells indicated that induction of ALB$^+$ cells from ALB$^-$ sorted cells was stimulated by HGF and OSM, and, to a lesser extent, by laminin, type IV collagen and type I collagen (Fig. 3B, upper graph). By contrast, HGF and OSM strongly inhibited the generation of ALB$^-$ cells from ALB$^+$ sorted cells. Laminin, type IV collagen and type I collagen-coated dishes had similar inhibitory effects on the generation of ALB$^-$ cells (Fig. 3B, lower graph). Interestingly, aFGF and bFGF, which induce hepatogenesis in ventral endoderm at E8 (Jung et al., 1999), had little effect on stem cell growth and differentiation in our culture system.

In addition to FACS-analyses we further examined the effect of HGF and OSM on stem cell cultures to determine in detail the mechanism by which they induce differentiation of hepatocyte-lineage cells. After 10 days culture of either ALB$^-$ or ALB$^+$ sorted cells, quantitative PCR was performed to examine the expression patterns of hepatocyte or cholangiocyte differentiation markers. In ALB$^-$ sorted cell cultures, HGF strongly induced ALB and αAT expression, and OSM induced G6P expression, which is normally activated at the mid-late gestational stage. TO, a marker for mature hepatocytes, expressed only in adult liver, could not be detected because of its much lower expression (Fig. 4A, left). Although HGF also induced expression of ALB and αAT in ALB$^+$ sorted cell cultures, it did not induce latter markers of hepatocyte differentiation, such as G6P and TO. By contrast, OSM efficiently induced the expression of G6P and TO, and promoted the maturation of differentiating hepatocytes (Fig. 4A, right). In cultures with either HGF or OSM, AFP expression was decreased in both ALB$^-$ and ALB$^+$ sorted cell cultures. Cholangiocyte marker gene expression was also suppressed in cultures of both cell types by HGF and OSM (Fig. 4B). The laminin, type IV collagen and type I collagen promoted the expression of hepatocyte marker genes in both ALB$^-$ and ALB$^+$ cell cultures. Their effects, however, were not as strong as those of HGF and OSM, because relatively high expression of hepatocyte-differentiation marker genes was not detected until 20 days of culture and, furthermore, the expression of TO was too low to be determined by quantitative analysis (data not shown).

These results demonstrated that HGF can initiate the primary differentiation of stem cells into ALB$^+$ hepatic precursors. HGF subsequently works as a mitogen to expand early-differentiating cells, while OSM inhibits their proliferation and promotes their differentiation into mature cells. Both HGF and OSM direct stem cells to the hepatocyte lineage, and also suppress development into the bile duct lineage. Several ECMs such as laminin, type IV collagen and type I collagen also induce differentiation of stem cells, in a similar manner to HGF and OSM, but their effect is much less dramatic than that of GFs. ECMs may function in the maintenance of stem cells and play a supportive role in their differentiation. Alternatively, ECMs may not affect stem cells directly, but instead could act on stem cell-derived precursors to promote their survival and differentiation.

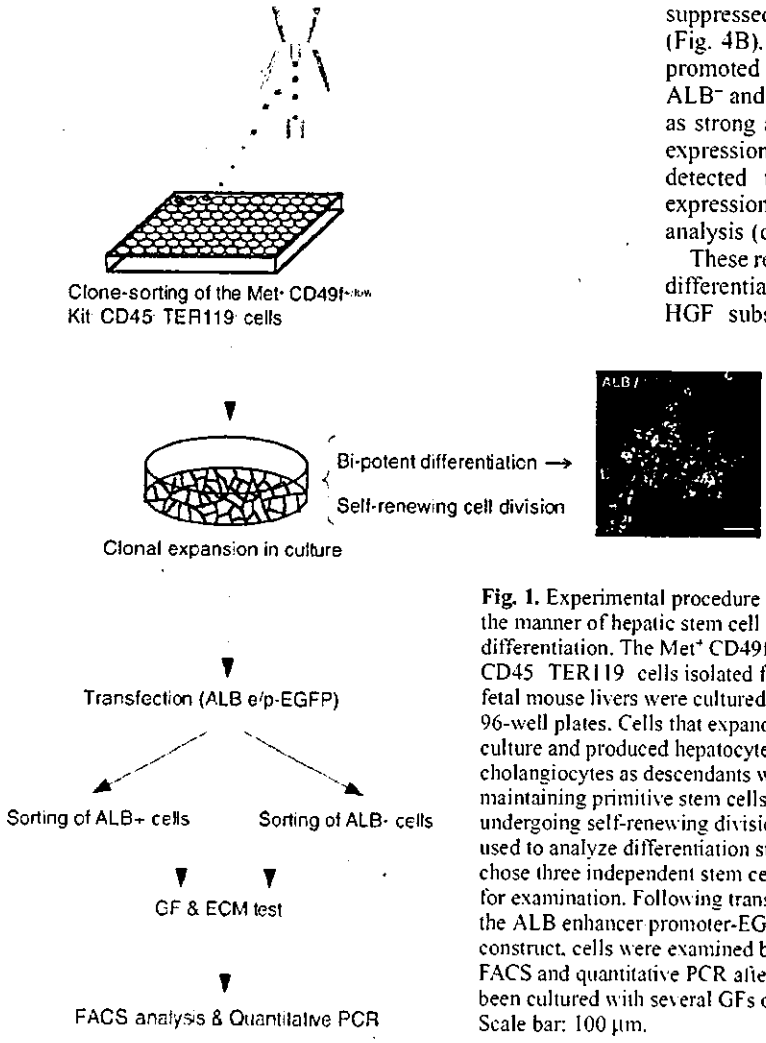

Fig. 1. Experimental procedure to elucidate the manner of hepatic stem cell differentiation. The Met$^+$ CD49f$^{+\,low}$ Kit$^-$ CD45$^-$ TER119$^-$ cells isolated from E13.5 fetal mouse livers were cultured clonally in 96-well plates. Cells that expanded in culture and produced hepatocytes and cholangiocytes as descendants while maintaining primitive stem cells undergoing self-renewing divisions were used to analyze differentiation status. We chose three independent stem cell clones for examination. Following transfection of the ALB enhancer promoter-EGFP construct, cells were examined by using FACS and quantitative PCR after they had been cultured with several GFs or ECMs. Scale bar: 100 μm.

The expression of C/EBPs changed dramatically during stem cell differentiation

To reveal the transcriptional control

of hepatocyte-differentiation from stem cells, we first examined the effect of HGF on the expression of C/EBPs, which are candidate key factors. C/EBP proteins comprise a family of transcription factors that have a bZIP structure, consisting of a DNA binding basic region and a leucine zipper dimerization domain (Lekstrom-Himes et al., 1998). They directly control the expression of genes encoding hepatocyte-specific proteins such as ALB and αAT (Costa et al., 1989; Maire et al., 1989; Trautwein et al., 1996). The expression of C/EBPα is particularly upregulated when hepatocytes shift from proliferation to the differentiation state (Rana et al., 1994; Runge et al., 1997). In the fetal liver of *Cebpa*$^{-/-}$ mice, hepatocytes exhibited biliary epithelial cell characteristics and many pseudoglandular structures appeared, suggesting an involvement of C/EBPα in directing differentiation of bi-potent hepatic stem cells along the hepatocyte-lineage (Tomizawa et al., 1998). As shown in Fig. 5A, the expression of C/EBPα in an original stem cell population was stimulated, in a dose-dependent manner, by HGF as well as laminin, type IV collagen and type I collagen. The differentiation of hepatocytes, represented by the expression of ALB, αAT and G6P, was also stimulated in stem cell cultures by high concentrations of HGF in the presence of ECMs (data not shown). By contrast, the expression of C/EBPβ was decreased by these culture conditions (Fig. 5A). HGF and ECMs were found to have little affect on the expression of C/EBPδ and C/EBPγ (data not shown).

After sorting and culture of ALB$^-$ and ALB$^+$ cells, C/EBPα was highly expressed in culture of ALB$^-$ cells with HGF, in which hepatic precursors actively differentiated from stem cells and proliferated, rather than ALB$^+$ cells (Fig. 5B). As C/EBPα expression was also synchronized with the expression of hepatocyte-differentiation genes such as ALB and αAT in culture of ALB$^-$ cells with HGF, as described in Fig. 4A (left), C/EBPα probably has a role in the primary differentiation of stem cells into hepatocyte-lineage cells.

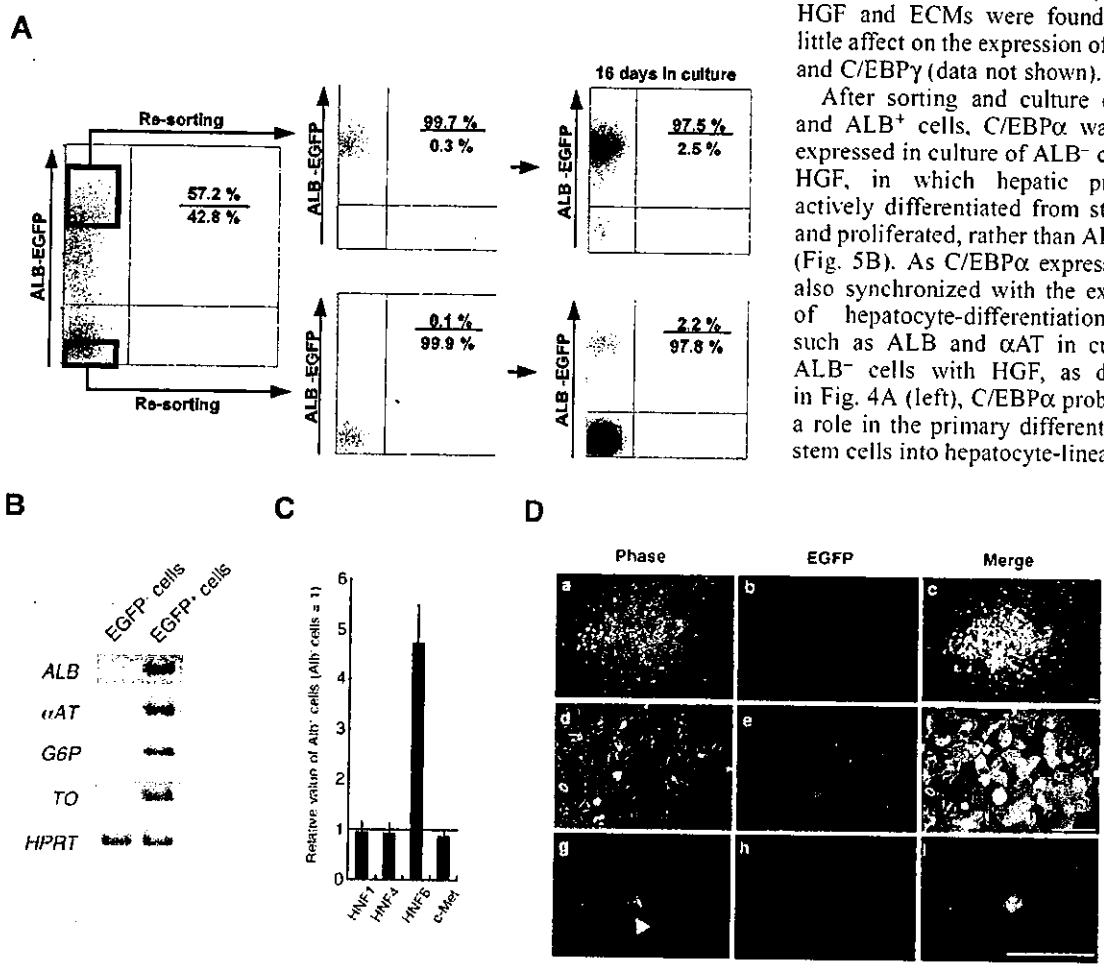

Fig. 2. Separation of differentiating ALB$^+$ cells from the stem cell population. (A) After gene transfer of the ALB enhancer promoter-EGFP construct into expanding stem cell populations, ALB$^+$ and ALB$^-$ cells were sorted restrictively using FACS. Immediate re-analysis of sorted cells showed purification of both ALB$^+$ and ALB$^-$ cells. After the culture of each sorted cell subpopulation for 16 days on type IV collagen-coated dishes, FACS analysis demonstrated that ALB$^-$ cells emerged from ALB$^+$ cells, and that ALB$^+$ cells emerged from ALB$^-$ cells. Percentages of fractionated cells are shown at the top of each panel. Establishment of the gate was based on the profile of the negative control. (B) Semi-quantitative RT-PCR analysis of sorted EGFP$^-$ (ALB$^+$) and EGFP$^+$ (ALB$^-$) cells. Note that ALB$^+$ sorted cells expressed hepatocyte-lineage markers, such as ALB, αAT, G6P and TO, at much higher levels than did ALB$^-$ cells. (C) Quantitative analysis of sorted ALB$^-$ cells using real-time quantitative PCR. All data were normalized to the value of ALB$^+$ sorted cells and fold-differences are shown. Representative data from a transfected stem cell clone are shown: three samples were examined for each protein. Data are mean±s.d. (D) (a-f) Several sorted ALB$^-$ cells could form clonal colonies including both ALB$^-$ and ALB$^+$ cells at day 20. (g-i) Moreover, ALB$^+$ sorted cells gave rise to ALB$^-$ cells even 1 day after the initiation of culture, and finally formed mosaic colonies similar to those from ALB$^-$ cells (black arrowhead in g, an original EGFP$^+$ cell; white arrowhead in g, a daughter cell). (a,d,g) Phase contrast. (b,e,h) Enhanced green fluorescence protein (EGFP) imaging. (c,f,i) Merge. d-f are magnifications of a-c, respectively. Scale bars: 100 μm.

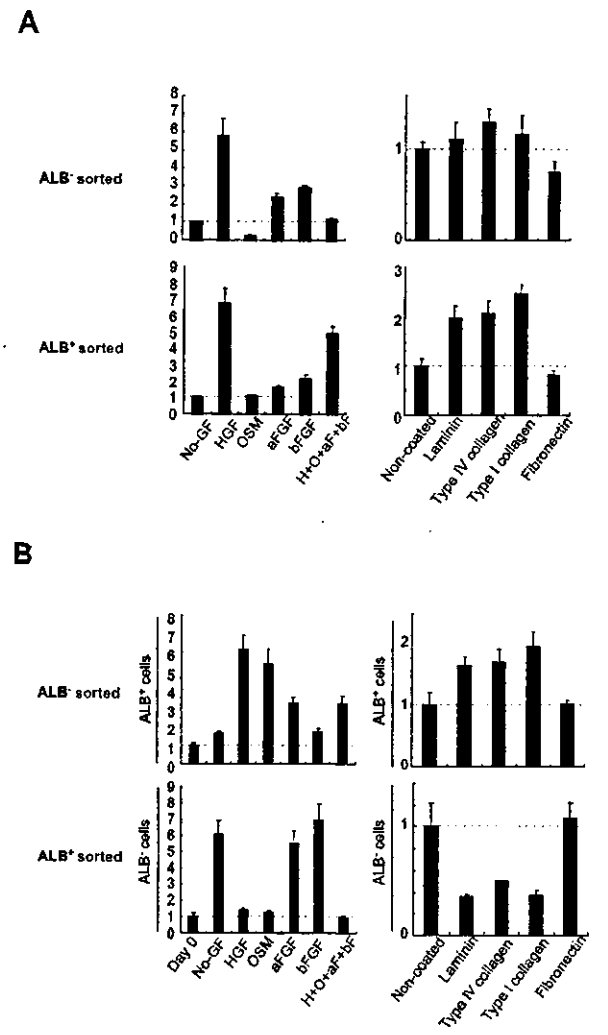

Fig. 3. Growth and differentiation of sorted ALB⁻ and ALB⁺ cells cultured with GFs and ECMs. FACS-sorted ALB⁻ and ALB⁺ cells were cultured separately. For the GF test, cells were cultured with or without HGF, OSM, aFGF, bFGF or a mixture of all GFs on type IV collagen-coated dishes. For the ECM test, cells were cultured on either non-coated, or laminin-, type IV collagen-, type I collagen- or fibronectin-coated dishes. After 10 days in culture, proliferation (A) and differentiation (B) of sorted cells were examined by cell counting (A) or FACS (B). Representative data from a transfected stem cell clone are shown; three samples were examined for each GF or ECM. Data are mean±s.d. (A) HGF strongly promoted the proliferation of both ALB⁻ and ALB⁺ sorted cells, whereas lesser effects were noted with OSM, aFGF and bFGF. OSM specifically suppressed the proliferation of ALB⁻ cells. For the ECMs, laminin, type IV collagen and type I collagen induced the proliferation of ALB⁻ cells, but to a lesser degree than HGF. All data were normalized to the value of no-GF (GF test) or a non-coated dish (ECM test) and fold-differences are shown. (B) FACS-analysis revealed that HGF and OSM have the potential to induce ALB⁻ cells from ALB⁻ sorted cells, and inhibit generation of ALB⁻ cells from ALB⁻ sorted cells. Laminin, type IV collagen and type I collagen possessed similar, but lesser, effects than did HGF and OSM. All data are normalized to the value at the day of sorting (day 0) (GF test) or to the value of a non-coated dish (ECM test) and fold differences are shown.

Lack of C/EBP proteins inhibits hepatocyte differentiation from stem cells

Using a retroviral gene transfer system, we expressed C/EBPα or β in stem cell cultures to examine their roles in differentiation. Transduced cells, however, stopped proliferating and died within a few days (data not shown). This suggested that too much C/EBP disrupted the homeostasis of hepatic stem cells. Therefore, we transduced cells with the retroviral vector GCsam-A-C/EBP-IRES-EGFP, which drives expression of both A-C/EBP and EGFP (Iwama et al., 2002), which disrupts the function of C/EBP proteins. A-C/EBP, a dominant-negative C/EBP that has the potential to antagonize all C/EBP members, is a 102 amino acid protein consisting of an N-terminal 9 amino acid Flag epitope, a 13 amino acid linker, a 31 amino acid designated acidic amphipathic helix, and a 49 amino acid leucine zipper domain of C/EBPα (Olive et al., 1996). The leucine zipper from A-C/EBP specifically interacts with endogenous C/EBP leucine zippers, and the N-terminal acidic extension forms a coiled coil with endogenous C/EBP basic regions. This heterodimeric coiled coil structure is much more stable than C/EBPα bound to DNA, and thus, the dominant-negative protein abolishes DNA binding of all endogenous C/EBP family members.

After transduction, EGFP-positive cells (98.2±0.8%; n=3) were sorted by FACS and then subjected to in vitro and in vivo assays. Stem cells expressing A-C/EBP failed to express hepatocyte-differentiation markers such as ALB, AFP, αAT, G6P and TO, even when cultured with both HGF and OSM, which normally induce hepatocyte differentiation (Fig. 6A). By contrast, the expression of CK19 and GGT, markers of cholangiocyte-differentiation, was relatively enhanced in cells expressing A-C/EBP. The expression of the transcription factors HNF1, HNF4 and Met was also activated by blocking C/EBP function, but this change was not significant. Interestingly, the expression of HNF6 was decreased in transduced cells, in a similar manner to other hepatocyte-differentiation markers (Fig. 6B). Both ALB immunocytochemistry and PAS staining also revealed that stem cells expressing A-C/EBP did not give rise to functionally mature hepatocytes expressing ALB and containing abundant glycogen stores (Fig. 6C). Instead of differentiation along the hepatocyte-lineage, cultured cells expressing A-C/EBP grew actively and formed a lot of large colonies including more than 100 cells in comparison with mock controls, suggesting activation or maintenance of self-renewal status (Fig. 6D). Sorted ALB⁺ and ALB⁻ cells were also transduced with the retroviral vector GCsam-A-C/EBP-IRES-NGFR and analyzed for differentiation potential into hepatocyte-lineage cells. In ALB⁺ cultured cells that expressed A-C/EBP (ALB⁺/NGFR⁺ cells) after FACS sorting, ALB⁻ cells emerged efficiently. Transduction of ALB⁻ cells, by contrast, strongly inhibited the generation of ALB⁺ cells (Fig. 6E). Taken together, these data indicate that the expression of C/EBPs, induced by HGF, OSM and ECMs, is a key event for primary differentiation of stem cells into bipotent precursors and hepatocyte-lineage cells, and that disruption of this transcriptional regulation leads to the maintenance of stem cell status, including self-renewal activity.

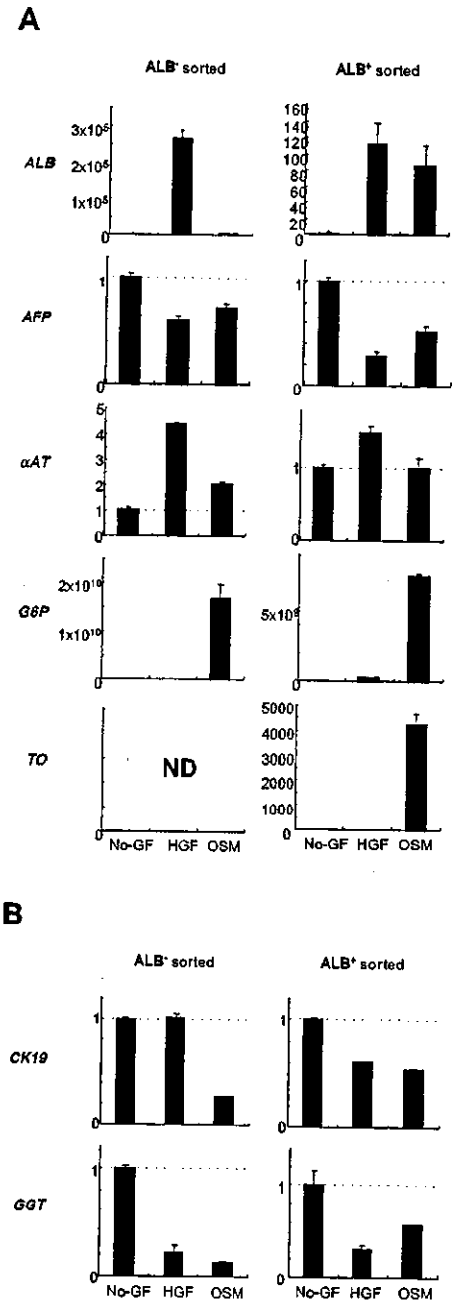

Fig. 4. Quantitative analysis of the effect of HGF and OSM on sorted ALB⁻ and ALB⁺ cells. FACS-sorted ALB⁻ and ALB⁺ cells were cultured separately with or without HGF or OSM on type IV collagen-coated dishes for 10 days. Then, quantitative PCR was performed to determine the expression of several hepatocyte or cholangiocyte marker genes. Representative data from a transfected stem cell clone are shown; three samples were examined for each GF. Data are mean±s.d. (A) In the ALB⁻ cell culture, HGF strongly induced ALB and αAT expression. The mid-latter marker G6P was induced exclusively by OSM, but TO expression was still not detected. In the ALB⁺ cell culture, however, OSM strongly induced G6P and TO expression. The expression of ALB in the ALB⁺ sorted cell cultures was also promoted by HGF and OSM, but its effects were not greater than in ALB⁻ cells. (B) Both HGF and OSM suppressed the expression of cholangiocyte marker genes such as CK19 and GGT in ALB⁻ and ALB⁺ sorted cell cultures. All data were normalized to the values of no-GF and fold differences are shown. ND, not detected.

DISCUSSION

To describe precisely sequential liver cell lineages derived from hepatic stem cells, we analyzed the differentiation status of purified stem cell populations in clonal experiments, after the exclusion of a number of differentiated cells and other cell lineages in the liver. Our previous report made it possible to isolate primary cells with stem cell activity from fetal mouse livers using FACS and culture them from single cells (Suzuki et al., 2002). Based on our present findings, we propose a possible lineage of stem cell differentiation in the developing liver (Fig. 7). Analysis of isolated stem cells revealed that initiation of the early differentiation of hepatocyte-lineage cells from stem cells was directly mediated by HGF. This identifies a novel function of HGF in liver development. In postnatal liver, HGF functions as an inducer of hepatocyte maturation (Hu et al., 1993; Kamiya et al., 2001), and in the regenerating liver, it stimulates proliferation of adult hepatocytes (Michalopoulos et al., 1984; Ishiki et al., 1992). HGF has been suggested to serve a role in the physiological activities of organ-specific stem cells owing to its ability to elicit repair and regeneration of many adult organs (Kawaida et al., 1994; Michalopoulos and DeFrances, 1997; Matsuda et al., 1997; Matsumoto et al., 1997; Stolz et al., 1999; Menke et al., 1999; Fausto, 2000; Xian et al., 2000; Sakamaki et al., 2002). Indeed, it stimulates differentiation and proliferation of human CD34-positive hematopoietic precursors and human embryonic stem cells (Galimi et al., 1994; Schuldiner et al., 2000). Thus, direct regulation by HGF may be a common mechanism among stem cells in multiple organs and critical for their differentiation and proliferation. We found that during the transition to ALB⁺ cells from ALB⁻ stem cells, HGF promotes production of ALB⁺ cells and allows them to proliferate efficiently. The ALB⁺ cells produced still possess the capacity to differentiate into cholangiocytes expressing CK19 and GGT in clonal cultures. Therefore, differentiating and proliferating ALB⁺ cells freshly generated from ALB⁻ stem cells may be equivalent to bi-potent hepatoblasts, which express several lineage markers and largely occupy the developing liver. Our previous data have also shown that isolated hepatic stem cells reside in the developing liver without expressing both hepatocyte and cholangiocyte lineage markers (Suzuki et al., 2000; Suzuki et al., 2002). Furthermore, such cells were much fewer in number than previously hypothesized and appear to decrease as gestation advances. These consolidated findings support our present hypothesis described above.

After the initiation of hepatic stem cell differentiation by HGF, OSM, which is produced by hematopoietic lineage cells, gave a permissive signal for differentiation of hepatic precursors to mature hepatocytes expressing G6P and TO. Both HGF and OSM strongly stimulated differentiation of ALB⁺ hepatic precursors into hepatocyte-lineage cells, and also prevented them from restoring the ALB⁻ phenotype and

differentiating into cholangiocyte-lineage cells. Several ECMs, such as laminin, type IV collagen and type I collagen, also induced differentiation of stem cells. Although ECMs are necessary for proliferation and differentiation of stem cells, their effects are likely to be only supportive for the differentiation of hepatocytes and cholangiocytes, based on their weaker potential for stem cell differentiation. Factors regulating cholangiocyte differentiation from stem cells or hepatic precursors were not identified in this study, suggesting that stem cell to cholangiocyte differentiation may be a favored pathway in stem cell differentiation, that does not require specific signals. Further intensive studies will be necessary to elucidate the manner of cholangiocyte differentiation from stem cells.

In ALB$^-$ cells generated from ALB$^+$ precursors in clonal cultures, both CK19$^+$ cholangiocyte-lineage cells and ALB$^-$ CK19$^-$ cells that possess a stem cell phenotype were identified (data not shown). These results suggest that ALB expression early during the differentiation of stem cells is flexible and cells can flow between stem cells and ALB$^+$ hepatic precursors before they obtain gradual signals for differentiation first from HGF and secondarily from OSM. In hepatogenesis from the endoderm layer starting at E8, FGFs produced by cardiac mesoderm play a key role in the generation of ALB$^+$ cells (Jung et al., 1999). Our present data, however, showed that FGFs

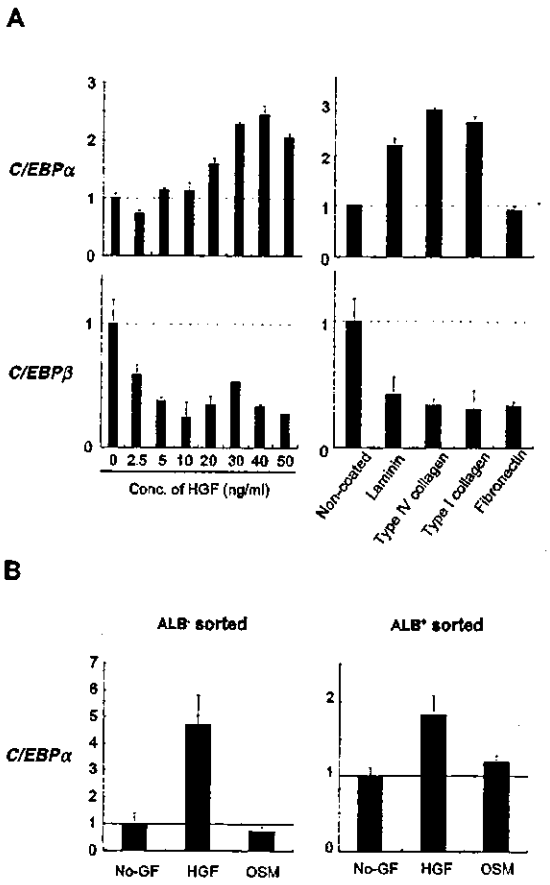

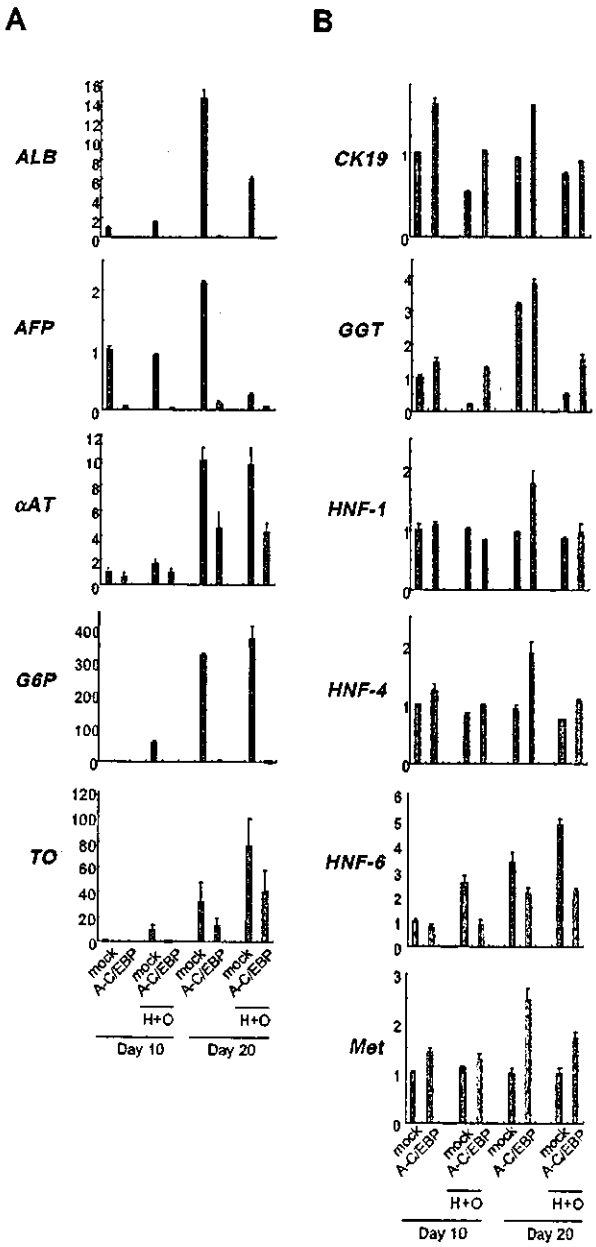

Fig. 5. HGF and several ECMs regulate C/EBP expression during stem cell differentiation. (A) When cells were cultured on type IV collagen-coated dishes for 8 days, C/EBPα expression was promoted in a dose-dependent manner by HGF, as well as by the presence of laminin, type IV collagen and type I collagen. By contrast, C/EBPβ expression was decreased in these culture conditions. All data were normalized to the expression values from 0 ng/ml (HGF) or non-coated dishes (ECM) and fold differences are shown. Representative data from a stem cell clone are shown: three samples were examined for each concentration of HGF or each ECM. Data are mean±s.d. (B) C/EBPα was highly expressed in ALB$^-$ and ALB$^+$ sorted cells cultured with HGF for 10 days. Its expression was promoted exclusively in the transition of ALB$^-$ cells to ALB$^-$ hepatic precursors induced by HGF. All data were normalized to the value of no-GF and fold differences are shown. Representative data from a transfected stem cell clone are shown: three samples were examined for each GF. Data are mean±s.d.

have much smaller effects on the transition from ALB⁻ stem cells to ALB⁺ cells. The E13.5 fetal mouse livers that we used for isolating stem cells had already been apart from cardiac mesoderm, indicating that FGFs should have finished their role in early liver development by this stage. A few cells receiving no signals from cardiac mesoderm or other lining mesenchymal cells in early hepatogenesis may be maintained in an undifferentiated state until the E13.5 mid-fetal stage. FGFs may directly induce the differentiation of hepatocytes and/or ALB⁺ hepatic precursors from foregut endoderm, but HGF stimulates the differentiation of dormant stem cells preserved in developing livers. A number of factors are likely to work mutually as inducers or repressors of liver organogenesis based on subtle timing.

C/EBP proteins regulate liver-specific gene expression and cell proliferation (Costa et al., 1989; Maire et al., 1989; Rana et al., 1994; Trautwein et al., 1996; Soriano et al., 1998; Greenbaum et al., 1998). In particular, C/EBPα is highly expressed in quiescent hepatocytes and positively regulates hepatocyte-specific gene expression, such as ALB and αAT (Costa et al., 1989; Maire et al., 1989; Rana et al., 1994; Runge et al., 1997; Soriano et al., 1998). In the developing liver of C/EBPα knockout mice, a number of pseudoglandular structures that co-express antigens specific for hepatocytes and cholangiocytes were found in the liver parenchyma, but the formation of bile ducts was not affected (Tomizawa et al., 1998). These data demonstrated that C/EBPα is an important regulator of hepatocyte differentiation, but not of cholangiocytes in either liver development or regeneration. In the results presented here, C/EBPα expression was highly induced during the progression of hepatocyte differentiation from ALB⁻ stem cells to ALB⁺ hepatic precursors by HGF. We suggest that HGF directly regulates the expression of C/EBPα, which plays a crucial role in the transition of stem cells to ALB⁺ hepatic precursors. C/EBPβ is also a liver enriched transcription factor (Descombes et al., 1990), which, similar to C/EBPα, is involved in the regulation of liver-specific genes such as ALB (Trautwein et al., 1996). In the transition

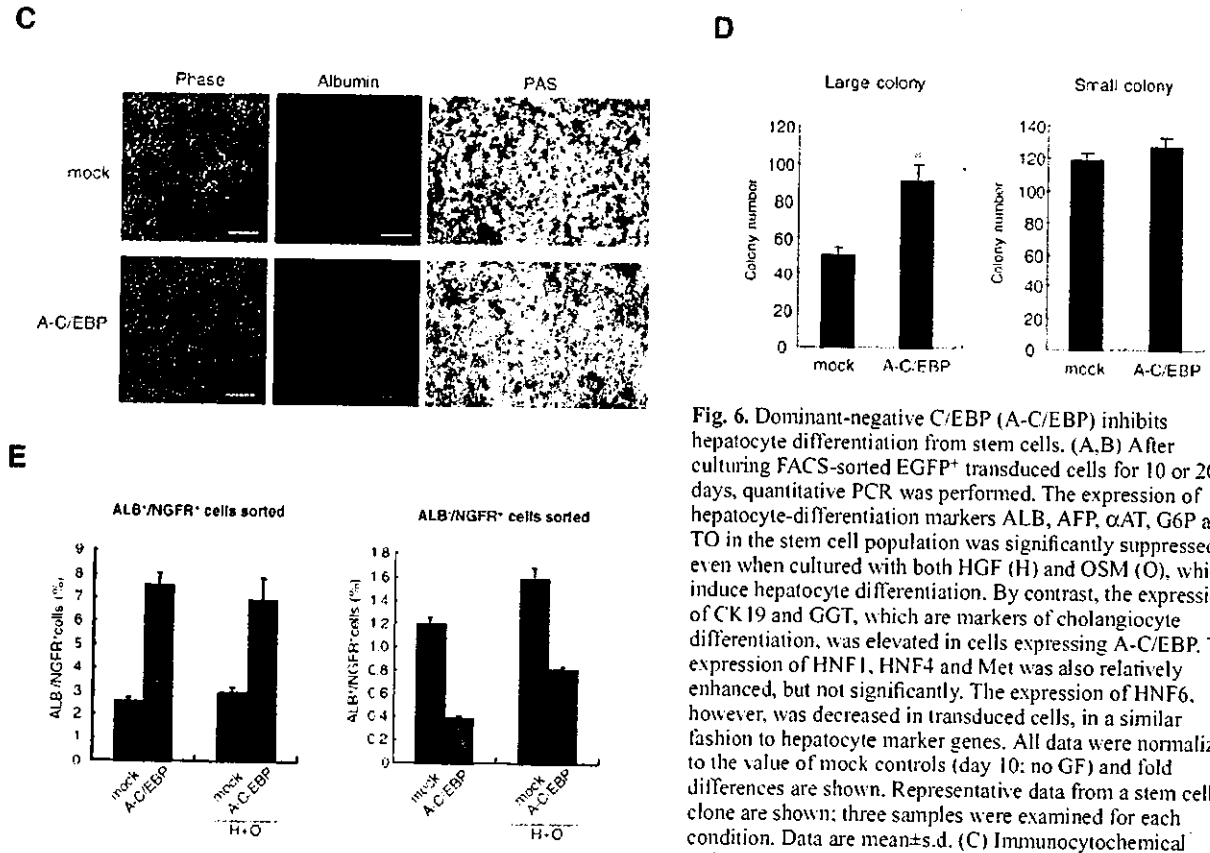

Fig. 6. Dominant-negative C/EBP (A-C/EBP) inhibits hepatocyte differentiation from stem cells. (A,B) After culturing FACS-sorted EGFP⁺ transduced cells for 10 or 20 days, quantitative PCR was performed. The expression of hepatocyte-differentiation markers ALB, AFP, αAT, G6P and TO in the stem cell population was significantly suppressed even when cultured with both HGF (H) and OSM (O), which induce hepatocyte differentiation. By contrast, the expression of CK19 and GGT, which are markers of cholangiocyte differentiation, was elevated in cells expressing A-C/EBP. The expression of HNF1, HNF4 and Met was also relatively enhanced, but not significantly. The expression of HNF6, however, was decreased in transduced cells, in a similar fashion to hepatocyte marker genes. All data were normalized to the value of mock controls (day 10: no GF) and fold differences are shown. Representative data from a stem cell clone are shown; three samples were examined for each condition. Data are mean±s.d. (C) Immunocytochemical staining of ALB and PAS-staining were performed on cells expressing EGFP (mock) or A-C/EBP at day 20. In cells expressing A-C/EBP, few cells were positive for ALB and stored glycogen. (counterstain: Hematoxylin). (D) After culture of sorted EGFP (mock) or A-C/EBP-expressing cells for 5 days in clonal density cultures (5×10^2 cells/well in six-well plates), the number of large (>100 cells in a colony) and small colonies was counted (n=6). The number of large colonies was increased when cells were transduced with A-C/EBP. Data are mean±s.d. (*P<0.005). (E) After transduction of FACS-sorted ALB⁺ or ALB⁻ cells by A-C/EBP-NGFR and culture of each cell population for 14 days, ALB⁺/NGFR⁺ cells or ALB⁻/NGFR⁺ cells were sorted separately and cultured with or without HGF and OSM for 10 days (plating density is 1×10^3 cells/cm^2). Then, the generation of ALB⁻ cells from ALB⁺/NGFR⁺ sorted cells and the generation of ALB⁺ cells from ALB⁻/NGFR⁺ sorted cells was examined by using FACS. Compared with mock controls, cells expressing A-C/EBP failed to maintain ALB expression in ALB⁺ sorted cells and were unable to generate ALB⁻ cells from ALB⁻ sorted cells. Representative data from a transfected stem cell clone are shown; three samples were examined for each condition. Data are mean±s.d. Scale bars: 100 μm.

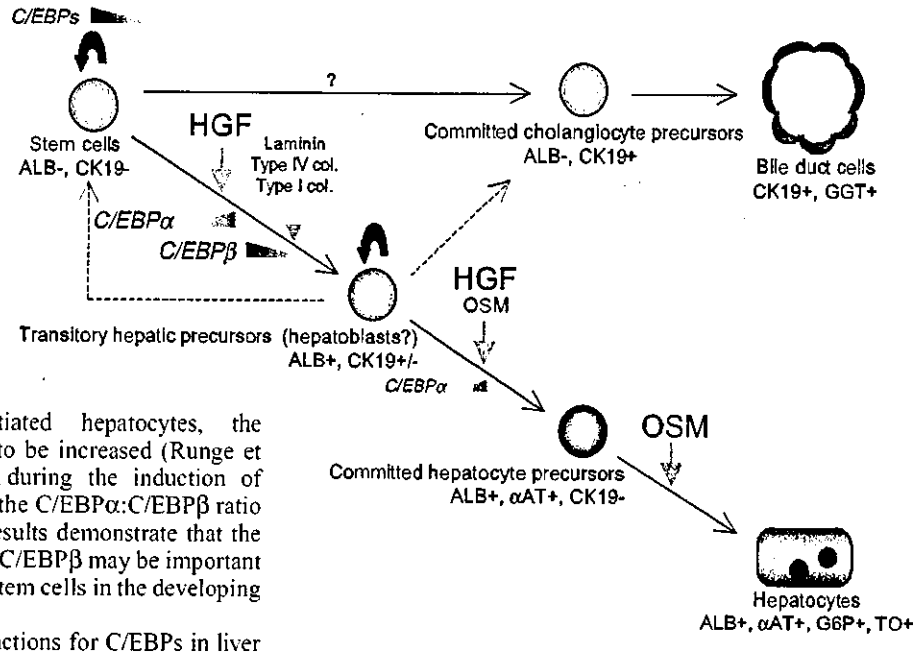

Fig. 7. Summarized possible mechanism for hepatic stem cell differentiation. Because early-generated ALB$^+$ cells can proliferate exclusively and differentiate into cholangiocyte-lineage cells, we speculate that transitory hepatic precursors expressing ALB exist in the developing liver and they are equivalent to bi-potent hepatoblasts.

from proliferating to differentiated hepatocytes, the C/EBPα:C/EBPβ ratio was found to be increased (Runge et al., 1997). In the present study, during the induction of hepatocyte-differentiation by HGF, the C/EBPα:C/EBPβ ratio was also highly increased. These results demonstrate that the relative proportions of C/EBPα and C/EBPβ may be important for hepatocyte differentiation from stem cells in the developing liver.

Using knockout mice, several functions for C/EBPs in liver development have been identified (Wang et al., 1995; Soriano et al., 1998; Tomizawa et al., 1998). However, as redundancy exists among C/EBP family members, their intrinsic roles in liver development remain to be clarified. For example, liver cells in C/EBPα knockout mice could differentiate into hepatocytes when they were cultured on Matrigel (Soriano et al., 1998), suggesting that partial redundancy with other C/EBP proteins exists. To eliminate these complicated interpretations, we used the dominant-negative A-C/EBP to abolish endogenous DNA binding of all C/EBP family members. The expression of A-C/EBP in ALB$^-$ stem cells resulted in semi-complete inhibition of the generation of hepatocyte-lineage cells, even in cultures including both HGF and OSM. In addition, A-C/EBP expression in ALB$^+$ cells advanced the transition to ALB$^-$ cells. These findings, collectively, show that the C/EBP family, especially C/EBPα and β, which are directly regulated by HGF, are required for the early steps in hepatic stem cell differentiation. In addition to inhibiting differentiation, lack of all C/EBP functions in stem cells enhances their self-renewal divisions in culture. In the developing liver, however, the number of stem cells is very low and their proliferation is restricted, even with the low expression of C/EBP proteins. Thus, other mechanisms may exist to maintain their quiescent status in liver development.

A number of molecular events in the differentiation of hepatic stem cells, such as the interaction of C/EBPs and other elements, are required for the determination of hepatocyte or cholangiocyte lineage. C/EBPα-mediated growth arrest is known to require interaction with p21, a cyclin-dependent kinase (CDK) inhibitor and CDK2 (Timchenko et al., 1997; Harris et al., 2001). This mechanism may be involved in OSM-mediated growth arrest of hepatic precursors, in order to then induce differentiation into mature hepatocytes. Because such growth inhibition is irrelevant to the transcriptional activity of C/EBPα (Harris et al., 2001), another mechanism should exist to control transcription of genes important for liver development. Actually, in the transcriptional control regions of ALB and αAT, liver-enriched transcription factors such as HNF1 (Baumhueter et al., 1990), HNF3 and HNF4 (Costa et al., 1989), and widely distributed proteins such as activator protein 1 (AP1) (Hu et al., 1994) bind to regulate these genes along with C/EBP proteins. The currently proposed cascade of sequential transcriptional control of hepatic stem cell differentiation, however, is still unreliable. Our present results show that HNF6 was expressed more highly in ALB$^+$ cells than ALB$^-$ cells during the early differentiation of stem cells, and HNF6 expression was also suppressed when stem cell differentiation was inhibited by dominant-negative C/EBP proteins. The HNF6-binding sequence, in fact, is present in the promoter regions of several hepatocyte-enriched genes, such as αAT, AFP, cytochrome P450, GLUT2 and TO (Samadani et al., 1996; Tan et al., 2002). Thus, HNF6 may be one possible candidate involved in the early transition of stem cells to hepatic precursors, and its expression may be regulated by C/EBPs. In *Hnf6*$^{-/-}$ mice, abnormalities of the intrahepatic and extrahepatic bile ducts and of the gallbladder were observed (Clotman et al., 2002). These data suggest that HNF6 is essential for differentiation and maturation of biliary lineage cells rather than hepatocytes. However, in the E13.5 developing liver of these mice a number of cytokeratin-positive biliary lineage cells emerged compared to normal mice, suggesting that HNF6 regulates not only morphogenesis of biliary tract but turning point of the differentiation of primitive hepatic stem cells.

A precise description of stem cell differentiation would allow the control of hepatocyte differentiation and the induction of liver regeneration by manipulating the endogenous stem cell compartment. Our clonal culture assay with hepatic stem cells should reveal the mechanism that regulates their self-renewal potential and the signals that restrict their proliferation and differentiation in the developing liver. Exploring diverse gene programs activated in stem cells or differentiating cells should provide a molecular framework

for future research into liver development. Key elements of stem cells, such as quiescent status and pluripotency, would be elucidated by comparing hepatic stem cells with other tissue-derived stem cells. The prospective isolation and characterization of stem cells is required for better understanding what exactly a stem cell is and what it does.

We thank N. Ukawa, M. Mori and Y. Jinzenji for technical support, and Y. Morita for FACS operation. This work was supported by Grants-in-Aid for Scientific Research from the Ministry of Education, Science and Culture of Japan (14207046, 12557096) and JSPS Research Fellowship for Young Scientists. This work was also supported by a grant from NISSAN Science Foundation.

REFERENCES

Baumhueter, S., Mendel, D. B., Conley, P. B., Kuo, C. J., Turk, C., Graves, M. K., Edwards, C. A., Courtois, G. and Crabtree, G. R. (1990). HNF-1 shares three sequence motifs with the POU domain proteins and is identical to LF-B1 and APF. *Genes Dev.* **4**, 372-379.

Clotman, F., Lannoy, V. J., Reber, M., Cereghini, S., Cassiman, D., Jacquemin, P., Roskams, T., Rousseau, G. G. and Lemaigre, F. P. (2002). The onecut transcription factor HNF6 is required for normal development of the biliary tract. *Development* **129**, 1819-1828.

Costa, R. H., Grayson, D. R. and Darnell, J. E., Jr (1989). Multiple hepatocyte-enriched nuclear factors function in the regulation of transthyretin and alpha 1-antitrypsin genes. *Mol. Cell. Biol.* **9**, 1415-1425.

Descombes, P., Chojkier, M., Lichtsteiner, S., Falvey, E. and Schibler, U. (1990). LAP, a novel member of the C/EBP gene family, encodes a liver-enriched transcriptional activator protein. *Genes Dev.* **4**, 1541-1551.

Fausto, N. (2000). Liver regeneration. *J. Hepatol.* **32**, 19-31.

Galimi, F., Bagnara, G. P., Bonsi, L., Cottone, E., Follenzi, A., Simeone, A. and Comoglio, P. M. (1994). Hepatocyte growth factor induces proliferation and differentiation of multipotent and erythroid hemopoietic progenitors. *J. Cell Biol.* **127**, 1743-1754.

Greenbaum, L. E., Li, W., Cressman, D. E., Peng, Y., Ciliberto, G., Poli, V. and Taub, R. (1998). CCAAT enhancer- binding protein beta is required for normal hepatocyte proliferation in mice after partial hepatectomy. *J. Clin. Invest.* **102**, 996-1007.

Harris, T. E., Albrecht, J. H., Nakanishi, M. and Darlington, G. J. (2001). CCAAT enhancer-binding protein-alpha cooperates with p21 to inhibit cyclin-dependent kinase-2 activity and induces growth arrest independent of DNA binding. *J. Biol. Chem.* **276**, 29200-29209.

Hu, J. and Isom, H. C. (1994). Suppression of albumin enhancer activity by H-ras and AP-1 in hepatocyte cell lines. *Mol. Cell. Biol.* **14**, 1531-1543.

Hu, Z., Evarts, R. P., Fujio, K., Marsden, E. R. and Thorgeirsson, S. S. (1993). Expression of hepatocyte growth factor and c-met genes during hepatic differentiation and liver development in the rat. *Am. J. Pathol.* **142**, 1823-1830.

Ishiki, Y., Ohnishi, H., Muto, Y., Matsumoto, K. and Nakamura, T. (1992). Direct evidence that hepatocyte growth factor is a hepatotrophic factor for liver regeneration and has a potent antihepatitis effect in vivo. *Hepatology* **16**, 1227-1235.

Iwama, A., Osawa, M., Hirasawa, R., Uchiyama, N., Kaneko, S., Onodera, M., Shibuya, K., Shibuya, A., Vinson, C., Tenen, D. G. et al. (2002). Reciprocal roles for CCAAT enhancer binding protein (C/EBP) and PU.1 transcription factors in Langerhans cell commitment. *J. Exp. Med.* **195**, 547-558.

Jacquemin, P., Durviaux, S. M., Jensen, J., Godfraind, C., Gradwohl, G., Guillemot, F., Madsen, O. D., Carmeliet, P., Dewerchin, M., Collen, D. et al. (2000). Transcription factor hepatocyte nuclear factor 6 regulates pancreatic endocrine cell differentiation and controls expression of the proendocrine gene ngn3. *Mol. Cell. Biol.* **20**, 4445-4454.

Jung, J., Zheng, M., Goldfarb, M. and Zaret, K. S. (1999). Initiation of mammalian liver development from endoderm by fibroblast growth factors. *Science* **284**, 1998-2003.

Kamiya, A., Kinoshita, T., Ito, Y., Matsui, T., Morikawa, Y., Senba, E., Nakashima, K., Taga, T., Yoshida, K., Kishimoto, T. et al. (1999). Fetal liver development requires a paracrine action of oncostatin M through the gp130 signal transducer. *EMBO J.* **18**, 2127-2136.

Kamiya, A., Kinoshita, T. and Miyajima, A. (2001). Oncostatin M and hepatocyte growth factor induce hepatic maturation via distinct signaling pathways. *FEBS Lett.* **492**, 90-94.

Kaneko, S., Onodera, M., Fujiki, Y., Nagasawa, T. and Nakauchi, H. (2001). The simplified retroviral vector GCsap with murine stem cell virus long terminal repeat allows high and continued expression of enhanced green fluorescent protein by human hematopoietic progenitors engrafted in non-obese diabetic / severe combined immunodeficiency mice. *Hum. Gene Ther.* **12**, 35-44.

Kawaida, K., Matsumoto, K., Shimazu, H. and Nakamura, T. (1994). Hepatocyte growth factor prevents acute renal failure and accelerates renal regeneration in mice. *Proc. Natl. Acad. Sci. USA* **91**, 4357-4361.

Kinoshita, T., Sekiguchi, T., Xu, M. J., Ito, Y., Kamiya, A., Tsuji, K., Nakahata, T. and Miyajima, A. (1999). Hepatic differentiation induced by oncostatin M attenuates fetal liver hematopoiesis. *Proc. Natl. Acad. Sci. USA* **96**, 7265-7270.

Lekstrom-Himes, J. and Xanthopoulos, K. G. (1998). Biological role of the CCAAT/enhancer-binding protein family of transcription factors. *J. Biol. Chem.* **273**, 28545-28548.

Maire, P., Wuarin, J. and Schibler, U. (1989). The role of cis-acting promoter elements in tissue-specific albumin gene expression. *Science* **244**, 343-346.

Matsuda, Y., Matsumoto, K., Yamada, A., Ichida, T., Asakura, H., Komoriya, Y., Nishiyama, E. and Nakamura, T. (1997). Preventive and therapeutic effects in rats of hepatocyte growth factor infusion on liver fibrosis cirrhosis. *Hepatology* **26**, 81-89.

Matsumoto, K. and Nakamura, T. (1997). Hepatocyte growth factor (HGF) as a tissue organizer for organogenesis and regeneration. *Biochem. Biophys. Res. Commun.* **239**, 639-644.

Menke, A., Yamaguchi, H., Giehl, K. and Adler, G. (1999). Hepatocyte growth factor and fibroblast growth factor 2 are overexpressed after cerulein-induced acute pancreatitis. *Pancreas* **18**, 28-33.

Michalopoulos, G. K. and DeFrances, M. C. (1997). Liver regeneration. *Science* **276**, 60-66.

Michalopoulos, G., Houck, K. A., Dolan, M. L. and Leutteke, N. C. (1984). Control of hepatocyte replication by two serum factors. *Cancer Res.* **44**, 4414-4419.

Miller, A. D. (1996). Cell-surface receptors for retroviruses and implications for gene transfer. *Proc. Natl. Acad. Sci. USA* **93**, 11407-11413.

Olive, M., Williams, S. C., Dezan, C., Johnson, P. F. and Vinson, C. (1996). Design of a C/EBP-specific, dominant-negative bZIP protein with both inhibitory and gain-of-function properties. *J. Biol. Chem.* **271**, 2040-2047.

Pinkert, C. A., Ornitz, D. M., Brinster, R. L. and Palmiter, R. D. (1987). An albumin enhancer located 10 kb upstream functions along with its promoter to direct efficient, liver-specific expression in transgenic mice. *Genes Dev.* **1**, 268-276.

Rana, B., Mischoulon, D., Xie, Y., Bucher, N. L. and Farmer, S. R. (1994). Cell-extracellular matrix interactions can regulate the switch between growth and differentiation in rat hepatocytes: reciprocal expression of C/EBP alpha and immediate-early growth response transcription factors. *Mol. Cell. Biol.* **14**, 5858-5869.

Rossi, J. M., Dunn, N. R., Hogan, B. L. and Zaret, K. S. (2001). Distinct mesodermal signals, including BMPs from the septum transversum mesenchyme, are required in combination for hepatogenesis from the endoderm. *Genes Dev.* **15**, 1998-2009.

Runge, D., Runge, D. M., Bowen, W. C., Locker, J. and Michalopoulos, G. K. (1997). Matrix induced re-differentiation of cultured rat hepatocytes and changes of CCAAT enhancer binding proteins. *J. Biol. Chem.* **378**, 873-881.

Sakamaki, Y., Matsumoto, K., Mizuno, S., Miyoshi, S., Matsuda, H. and Nakamura, T. (2002). Hepatocyte growth factor stimulates proliferation of respiratory epithelial cells during postpneumonectomy compensatory lung growth in mice. *Am. J. Respir. Cell Mol. Biol.* **26**, 525-533.

Samadani, U. and Costa, R. H. (1996). The transcriptional activator hepatocyte nuclear factor 6 regulates liver gene expression. *Mol. Cell. Biol.* **16**, 6273-6284.

Schuldiner, M., Yanuka, O., Itskovitz-Eldor, J., Melton, D. A. and Benvenisty, N. (2000). From the cover: effects of eight growth factors on the differentiation of cells derived from human embryonic stem cells. *Proc. Natl. Acad. Sci. USA* **97**, 11307-11312.

Shiojiri, N., Lemire, J. M. and Fausto, N. (1991). Cell lineages and oval cell progenitors in rat liver development. *Cancer Res.* **51**, 2611-2620.

Soriano, H. E., Kang, D. C., Finegold, M. J., Hicks, M. J., Wang, N. D., Harrison, W. and Darlington, G. J. (1998). Lack of C/EBP alpha gene expression results in increased DNA synthesis and an increased frequency

of immortalization of freshly isolated mice [correction of rat] hepatocytes. *Hepatology* **27**, 392-401.

Spagnoli, F. M., Amicone, L., Tripodi, M. and Weiss, M. C. (1998). Identification of a bipotential precursor cell in hepatic cell lines derived from transgenic mice expressing cyto-Met in the liver. *J. Cell Biol.* **143**, 1101-1112.

Stolz, D. B., Mars, W. M., Petersen, B. E., Kim, T. H. and Michalopoulos, G. K. (1999). Growth factor signal transduction immediately after two-thirds partial hepatectomy in the rat. *Cancer Res.* **59**, 3954-3960.

Suzuki, A., Zheng, Y. W., Kondo, R., Kusakabe, M., Takada, Y., Fukao, K., Nakauchi, H. and Taniguchi, H. (2000). Flow cytometric separation and enrichment of hepatic progenitor cells in the developing mouse liver. *Hepatology* **32**, 1230-1239.

Suzuki, A., Zheng, Y. W., Kaneko, S., Onodera, M., Fukao, K., Nakauchi, H. and Taniguchi, H. (2002). Clonal identification and characterization of self-renewing pluripotent stem cells in the developing liver. *J. Cell Biol.* **156**, 173-184.

Tan, Y., Adami, G. and Costa, R. H. (2002). Maintaining HNF6 expression prevents AdHNF3beta-mediated decrease in hepatic levels of Glut-2 and glycogen. *Hepatology* **35**, 790-798.

Timchenko, N. A., Harris, T. E., Wilde, M., Bilyeu, T. A., Burgess-Beusse, B. L., Finegold, M. J. and Darlington, G. J. (1997). CCAAT/enhancer binding protein alpha regulates p21 protein and hepatocyte proliferation in newborn mice. *Mol. Cell. Biol.* **17**, 7353-7361.

Tomizawa, M., Garfield, S., Factor, V. and Xanthopoulos, K. G. (1998). Hepatocytes deficient in CCAAT/enhancer binding protein alpha (C/EBP alpha) exhibit both hepatocyte and biliary epithelial cell character. *Biochem. Biophys. Res. Commun.* **249**, 1-5.

Trautwein, C., Rakemann, T., Pietrangelo, A., Plumpe, J., Montosi, G. and Manns, M. P. (1996). C/EBP-beta/LAP controls down-regulation of albumin gene transcription during liver regeneration. *J. Biol. Chem.* **271**, 22262-22270.

Wang, N. D., Finegold, M. J., Bradley, A., Ou, C. N., Abdelsayed, S. V., Wilde, M. D., Taylor, L. R., Wilson, D. R. and Darlington, G. J. (1995). Impaired energy homeostasis in C/EBP alpha knockout mice. *Science* **269**, 1108-1112.

Wilson, J. W., Groat, C. S. and Leduc, E. H. (1963). Histogenesis of the liver. *Ann. New York Acad. Sci.* **111**, 8-24.

Xian, C. J., Couper, R., Howarth, G. S., Read, L. C. and Kallincos, N. C. (2000). Increased expression of HGF and c-met in rat small intestine during recovery from methotrexate-induced mucositis. *Br. J. Cancer* **82**, 945-952.

Zaret, K. S. (2000). Liver specification and early morphogenesis. *Mech. Dev.* **92**, 83-88.

Paired Activating and Inhibitory Immunoglobulin-like Receptors, MAIR-I and MAIR-II, Regulate Mast Cell and Macrophage Activation

Katsumi Yotsumoto,[1,2] Yasushi Okoshi,[1,2] Kazuko Shibuya,[1,2] Satoshi Yamazaki,[1,2,3] Satoko Tahara-Hanaoka,[1,2,3] Shin-ichiro Honda,[1,2,3] Mitsujiro Osawa,[1] Asato Kuroiwa,[5] Yoichi Matsuda,[5] Daniel G. Tenen,[6] Atsushi Iwama,[1,6] Hiromitsu Nakauchi,[1,4] and Akira Shibuya[1,2,3]

[1]*Department of Immunology, Institute of Basic Medical Sciences, University of Tsukuba, Tsukuba, Ibaraki 305-8575, Japan*

[2]*Laboratory for Immune Receptor, RIKEN Research Center for Allergy and Immunology, Tsukuba, Ibaraki 305-0034, Japan*

[3]*Precursory Research for Embryonic Science and Technology and* [4]*Core Research for Evolutional Science and Technology, Japan Science and Technology Corporation, Tsukuba, Ibaraki 305-8575, Japan*

[5]*Laboratory of Cytogenetics, Division of Bioscience, Graduate School of Environmental Earth Science and Chromosome Research Unit, Faculty of Science, Hokkaido University, Kita-ku, Sapporo 060-0810, Japan*

[6]*Harvard Institute of Medicine, Harvard Medical School, Boston, MA 02115*

Abstract

Immune responses are regulated by opposing positive and negative signals triggered by the interaction of activating and inhibitory cell surface receptors with their ligands. Here, we describe novel paired activating and inhibitory immunoglobulin-like receptors, designated myeloid-associated immunoglobulin-like receptor (MAIR) I and MAIR-II, whose extracellular domains are highly conserved by each other. MAIR-I, expressed on the majority of myeloid cells, including macrophages, granulocytes, mast cells, and dendritic cells, contains the tyrosine-based sorting motif and the immunoreceptor tyrosine-based inhibitory motif-like sequences in the cytoplasmic domain and mediates endocytosis of the receptor and inhibition of IgE-mediated degranulation from mast cells. On the other hand, MAIR-II, expressed on subsets of peritoneal macrophages and B cells, associates with the immunoreceptor tyrosine-based activation motif-bearing adaptor DAP12 and stimulates proinflammatory cytokines and chemokine secretions from macrophages. Thus, MAIR-I and MAIR-II play important regulatory roles in cell signaling and immune responses.

Key words: ITAM • ITIM • innate immunity • DAP12 • myeloid cells

Introduction

The activating and inhibitory cell surface receptors play important regulatory roles in immune responses (1, 2). The immune inhibitory receptors are characterized by a consensus amino acid (aa)* sequence, immunoreceptor tyrosine-based inhibitory motif (ITIM), present in their cytoplasmic domains. The prototype six-aa sequence for ITIM is (I/V/L/S)-x-Y-x-x-(L/V), where x denotes any aa. Upon ligand binding, immune inhibitory receptors result in tyrosine phosphorylation, which provides a docking site for the recruitment of Src homology 2 (SH2)–containing cytoplas-

Address correspondence to Akira Shibuya, Laboratory for Immune Receptor, RIKEN Research Center for Allergy and Immunology, 3-1-1 Koyadai, Tsukuba, Ibaraki 305-0074, Japan. Phone: 81-29-836-9174; Fax: 81-29-836-9175; E-mail: ashibuya@md.tsukuba.ac.jp

The present address of M. Osawa, A. Iwama, and H. Nakauchi is the Laboratory of Stem Cell Therapy, Center for Experimental Medicine, The Institute of Medical Science, University of Tokyo, Tokyo, 108-8639 Japan.

*Abbreviations used in this paper: aa, amino acid; FISH, fluorescence in situ hybridization; ITAM, immunoreceptor tyrosine-based activation motif; ITIM, immunoreceptor tyrosine-based inhibitory motif; MAIR, myeloid-associated immunoglobulin-like receptor; MCP-1, monocyte chemoatractant protein 1; PIR, paired Ig-like receptor; RDA, representational difference analysis; RT, reverse transcription; SH2, Src homology 2; SHIP, SH2 domain–containing inositol-5–phosphatase.

mic phosphatases (3, 4), shutting down activation signals by dephosphorylation of intracellular substrates at the earliest steps of the activation response. An expanding family of immune inhibitory receptors has been identified on a variety of immune cell types (1).

Recent progress has further demonstrated that many of these immune inhibitory receptors pair with activating, as well as inhibitory, isoforms (2, 5), both of whose genes are located in small clusters on a chromosome (6). For example, the NK inhibitory receptor families KIR, CD94/NKG2, and Ly49, which recognize MHC class I ligands, contain both activating and inhibitory receptors within the families (7). The paired activating and inhibitory receptor families have also been identified on other cell types. The CD28 and CTLA4 expressed on T cells bind the same ligands (i.e., CD80 and CD86) yet deliver opposing positive and negative signals, respectively (8). Similarly, B and/or myeloid cells express paired receptor families, including human and murine Fcγ receptors (9, 10), murine paired Ig-like receptors (PIRs; references 11, 12) and possibly its human homologue, Ig-like transcripts (ILT; CD85; references 13–15), and signal regulatory proteins (16–18). In contrast to the inhibitory receptors, the activating receptors have a short cytoplasmic domain lacking ITIM but containing a charged aa residue in the transmembrane region, which is involved in association with immunoreceptor tyrosine-based activation motif (ITAM)–bearing adaptor transmembrane proteins, such as FcεRIγ or DAP12, or with DAP10 adaptors containing PI3 kinase binding motif (19, 20). Among these activating and inhibitory receptors, KIR, PIR, ILT, and signal regulatory proteins belong to the Ig supergene family, which is characterized by the extracellular portion containing Ig-like domain, in some cases binding the same ligands that are highly homologous to each other (2, 6). The genes encoding most of these receptors are located on human chromosome 19q13.4 or its syntenic region on murine chromosome 7 (6).

In the present investigation, we have identified novel paired activating and inhibitory Ig-like receptors, designated myeloid-associated immunoglobulin-like receptor (MAIR) I and MAIR-II, expressed on the majority of macrophages, granulocytes, dendritic cells, mast cells, and a subset of B cells. Here, we describe the molecular and functional characteristics of the MAIR.

Materials and Methods

Antibodies. Control rat and mouse IgGs, anti–mouse TCRβ, CD45R/B220, CD11b (Mac1), CD11c, Ly6G (Gr-1), CD21, CD23, and CD32/16 mAbs and DX-5 mAb were purchased from BD Biosciences; antiphosphotyrosine (4G10) and anti-FcεRIγ mAbs were purchased from Upstate Biotechnology; anti-Flag mAb was purchased from Sigma-Aldrich; anti-SHP-1, anti–SHP-2, and anti–SH 2 domain–containing inositol-5–phosphatase (SHIP) antibodies were purchased from Santa Cruz Biotechnology, Inc.; and rat IgE anti-DNP mAb was purchased from Zymed Laboratories. Anti-DAP12 polyclonal antibody was a gift from M. Ono (Ehime University School of Medicine, Ehime, Japan). TX-8 (anti–MAIR-I), TX-10 (anti–MAIR-I and MAIR-II), and TX-13 (anti–MAIR-II) mAbs were generated in our laboratory by fusing the Sp2/0 myeloma cell line with popliteal lymph node cells from rats that had been immunized by injection of Ba/F3 transfectants expressing the MAIR-I or MAIR-II, and each extracellular protein was fused with the Fc portion of human IgG into footpads, as described previously (21). $F(ab')_2$ fragments were prepared by digesting TX-8 and TX-13 mAbs with immobilized pepsin (10 mg IgG in 10 ml of 0.2 M sodium citrate, 0.15 M NaCl buffer, pH 3.5, with 2.5 ml of immobilized pepsin for 1 h at 37°C; Pierce Chemical Co.), and afterwards, by removing residual intact mAb by protein A affinity chromatography. Purity of the $F(ab')_2$ fragments were determined by SDS-PAGE.

Representational Difference Analysis (RDA) and cDNA Cloning. Total RNA was isolated using Isogen LS solution (Nippon Gene), and oligo(dT)-primed double-stranded cDNA was synthesized using a cDNA synthesis system (GIBCO BRL) according to the manufacturer's instructions. RDA was performed, as described previously (22), using day 14 fetal livers from wild-type and PU.1$^{-/-}$ mice. Full-length *MAIR-Ia* cDNA was cloned by screening of a macrophage cDNA library, using a cDNA fragment generated by RDA as a probe. Full-length *MAIR-Ib*, *MAIR-IIa*, and *MAIR-IIb* cDNAs were also isolated by screening the same cDNA library, using the extracellular domain of *MAIR-Ia* cDNA as a probe.

Northern Blot Analysis. *MAIR-I* cDNA was labeled with [^{32}P]dCTP using the Ready to Go DNA Labeling Beads (Amersham Biosciences). Membranes containing ~10 μg of total RNA in each lane from different mouse tissues were hybridized with the [^{32}P]dCTP–labeled cDNA probes at 68°C in modified Church's hybridization buffer (0.5 M Church's phosphate buffer, 7% SDS, and 1% BSA). The membranes were washed at 68°C for 1 h in Church's washing buffer (40 mM Church's phosphate buffer and 1% SDS) and developed by autoradiography.

Reverse Transcription(RT)–PCR. RNA was subjected to RT and PCR using *MAIR-I*–specific primers (5′-GCTGATAGGCATCCAGAGC-3′ and 5′-AAGGAGTCACAGGTAAAGGTC-3′), *MAIR-II*–specific primers (5′-TCGAGCCTTGAGAGTGGTAGAC-3′ and 5′-AGGAGCTGTGTTTAGGGACAG-3′), DAP12-specific primers (5′-GGCTCTGGAGCCCTCCTGGT-3′ and 5′-CTGTGTGTTGAGGTCACTG-3′), or *HPRT*-specific primers (5′-GCTGGTGAAAAGGACCTCT-3′ and 5′-CACAGGACTAGAACACCTGC-3′). The amount of cDNA was normalized by the quantitative PCR using TaqMan rodent GAPDH control reagent (Applied Biosystems; reference 23). Conditions used for PCR were as follows: 30 or 35 cycles of 20-s denaturation (94°C), 20-s annealing (55°C), and 30-s extension (72°C).

Fluorescence in Situ Hybridization (FISH). The direct R-banding FISH method was used for chromosomal assignment of the *MAIR-I* gene in mouse and rat. Preparation of R-banded chromosomes and FISH were performed, as described by Matsuda et al. (24) and Matsuda and Chapman (25).

Establishment of Transfectants Expressing MAIR-I or MAIR-II. The *MAIR-I* and *MAIR-II* cDNA tagged with the flag cDNA at the NH_2 terminus were subcloned into the pMX retroviral vectors (26). To generate site-directed MAIR-I mutant at residues Y^{233}, PCR primers, which contained a codon for F^{233} (TTT) instead of Y^{233} (TAT), were designed. BW5147, Ba/F3, and RAW cells stably expressing Flag-tagged MAIR-I and MAIR-II were established as described previously (27).

Serotonin-release Assay. Bone marrow cells obtained from the femur and tibia of adult Balb/c mice were cultured at a concen-

tration of 2 × 10^5 cells/ml in RPMI 1640 medium containing 10% FBS, 4 ng/ml mouse rIL-3 (BD Biosciences), and 10 ng/ml mouse rSCF (provided by KIRIN). The bone marrow–derived nonadherent cells were transferred weekly into new culture dishes over a 4–10-wk culture interval. Ig-E–mediated serotonin release assay was performed as described previously (28). In brief, bone marrow–derived mast cells were incubated with 5 μCi/ml [^{3}H]serotonin (5-[1,2-^{3}H(*N*)]-hydroxytryptamine creatinine sulfate; NEN Life Science Products) for 5 h at 37°C, washed, and reincubated for an additional 1 h to reduce background radioactivity. [^{3}H]Serotonin-loaded mast cells were plated in 96-well plates that contained 10 μl of rat IgE, 25 μg/ml anti-DNP mAb, and various concentrations of F(ab′)$_2$ fragments of rat anti–MAIR-I or control IgG, incubated for 30 min at 4°C, washed, and resuspended in 25 μl of culture medium. Antibody-primed mast cells were challenged with 25 μl of F(ab′)$_2$ fragments of 40 μg/ml rabbit anti–rat Ig antibody for 30–60 min at 37°C. The reactions were terminated by adding 50 μl of cold PBS. [^{3}H]Serotonin in the supernatants were measured by a liquid scintillation counter.

Internalization Assay. Peritoneal macrophages were incubated with biotin-labeled anti–MAIR-I mAb (TX-8), followed by allophycocyanin-labeled streptavidin at 4° or 37°C for 30 min. Cells were treated or not with 2.5% trypsin and analyzed by flow cytometry. Ba/F3 transfectants expressing Flag-tagged MAIR-I at the NH_2 terminus were incubated with anti-Flag mAb, followed by cross-linking with FITC-labeled anti–mouse IgG secondary antibody at 4°C. Cells were resuspended in RPMI 1640 containing 10% FBS, plated onto polylysine-precoated chamber slide (Lab-Tek II; Nunc) and incubated at 37°C for 30 min. Cells were centrifuged at 1,500 rpm for 5 min at 4°C, washed with PBS twice, and fixed with 3% paraformaldehyde. Cells were mounted with VECTASHIELD including DAPI (Vector) and analyzed under a confocal scanning laser microscope.

Biochemistry. BW5147 transfectants expressing Flag-tagged MAIR-I or -II were lysed in Tris-buffered saline (50 mM Tris and 15 mM NaCl, pH 8.0) containing 1% NP-40, protease inhibitors (1 mM PMSF and 20 Kallikrein inhibitor U/ml aprotinin), and phosphatase inhibitors (1 mM EGTA, 10 mM NaF, 1 mM $Na_4P_2O_7$, 0.1 mM β-glycerophosphate, and 1 mM Na_3VO_4). To examine *N*-glycosylation of MAIR-I, lysates of BW5147 transfectants expressing Flag-tagged MAIR-I were immunoprecipitated with anti-Flag mAb or control Ig and treated or not with *N*-glycosidase F (Boehringer) using the conditions recommended by the manufacturers. To examine tyrosine phosphorylation of MAIR-I or association of MAIR-I with phosphatases, mast cells were stimulated or not with 100 mM sodium pervanadate for 10 min at 37°C. Cells were lysed in 1% digitonin (Sigma-Aldrich) buffer (0.12% Triton X-100; Katayama Pure Chemical), 150 mM NaCl, 20 mM triethanolamine (Katayama Pure Chemical), or 1% NP-40 buffer, containing the protease and phosphatase inhibitors. For analysis of association of MAIR-II with DAP12 or FcεRIγ, 293T or RAW transfectants expressing MAIR-II or B cells separated from spleen cells were lysed in 1% digitonin buffer, and cell lysates were immunoprecipitated with control Ig, anti-DAP12, or anti-FcεRIγ.

Lysates or immunoprecipitates were separated by SDS-PAGE, transferred (100 V, 1 h in 25 mM Tris, 195 mM glycine, and 20% methanol) to PVDF membranes (Immobilon-P; Millipore). Membranes were incubated overnight in Tris-buffered saline containing 0.5% Tween 20, $MgCl_2$, and 3% BSA at 4°C, and incubated with primary antibodies (1 μg/ml in Tris-buffered saline with 3% BSA) for 2 h at room temperature. Proteins were detected by using HRP-conjugated goat anti–mouse, anti–rat, or anti–rabbit Igs (Amersham Biosciences), and were developed with SuperSignal CL-HRP substrate (Pierce Chemical Co.). Chemiluminescences were detected by autoradiograph or image analyzer (LAS model 1000 mini; Fuji Film).

ELISA. RAW cells expressing Flag-tagged MAIR-II or peritoneal macrophages derived from C57BL/6 mice were pretreated with anti-CD32/16 (FcγR) to block Fcγ receptors, stimulated with plastic-coated control Ig, anti-Flag, or anti–MAIR-II mAb, and cultured for 24 or 48 h. TNF-α, IL-6, and monocyte chemoatractant protein 1 (MCP-1) concentrations in culture supernatants were measured using an ELISA kit (eBioscience) according to the manufacturer's instructions.

Results

Cloning and Molecular Characteristics of MAIR-I and MAIR-II. To identify novel genes involved in immune responses by myeloid cells, we performed representational differential analysis (RDA), which is a PCR-based subtractive hybridization, using day 14 fetal livers from PU.1$^{-/-}$ mice lacking myeloid cells and control littermates. We identified several cDNA clones unique to myeloid cells. Full-length cDNAs were cloned by screening a macrophage cDNA library. The predicted aa sequence demonstrates that the protein encoded by one of these cDNAs is a type-1 transmembrane protein with a 27-aa leader sequence, a 152-aa extracellular domain, a 23-aa transmembrane domain, and a 112-aa cytoplasmic region (Fig. 1 A). A pair of cysteine residues in the extracellular domain is flanked by consensus sequences for one Ig-like domain, indicating that the protein, designated MAIR-Ia, is a member of the Ig superfamily. The extracellular domain has one potential site for N-linked glycosylation, suggesting that MAIR-Ia is a glycoprotein. The cytoplasmic domain contains the five tyrosines at residues 233, 258, 270, and 299. Among these tyrosines, the residues at 258 and 270 may consist of ITIM-like sequences (VEY^{258}STL and LHY^{270}SSV, respectively) based on the consensus sequence for ITIMs (I/V/L/SxYxxL/V), suggesting that MAIR-I may recruit protein tyrosine phosphatases and mediate inhibitory signals. We found that the motif Y^{233}VNL is also a consensus sequence involved in receptor internalization (29, 30).

To examine whether MAIR-Ia is a member of paired activating and inhibitory receptors, we further screened the macrophage cDNA library using the cDNA encoding extracellular domain of MAIR-Ia as a probe. We identified a clone encoding the protein, designated MAIR-IIa, which contains one Ig-like domain with 92% aa identity to that of MAIR-Ia in extracellular domain, a transmembrane region with a charged (Lys aa) and a short (20 aa) cytoplasmic tail (Fig. 1, A and B). In addition, we found the isoforms of MAIR-Ia and MAIR-IIa, designated MAIR-Ib and MAIR-IIb, which contain additional four and two aas, respectively, in the extracellular domain. These are alternate splicing variants of *MAIR-Ia* and *MAIR-IIa*, as suggested by the genomic DNA sequence of *MAIR-I* and *MAIR-II* (unpublished data). Southern blot analysis of murine genomic

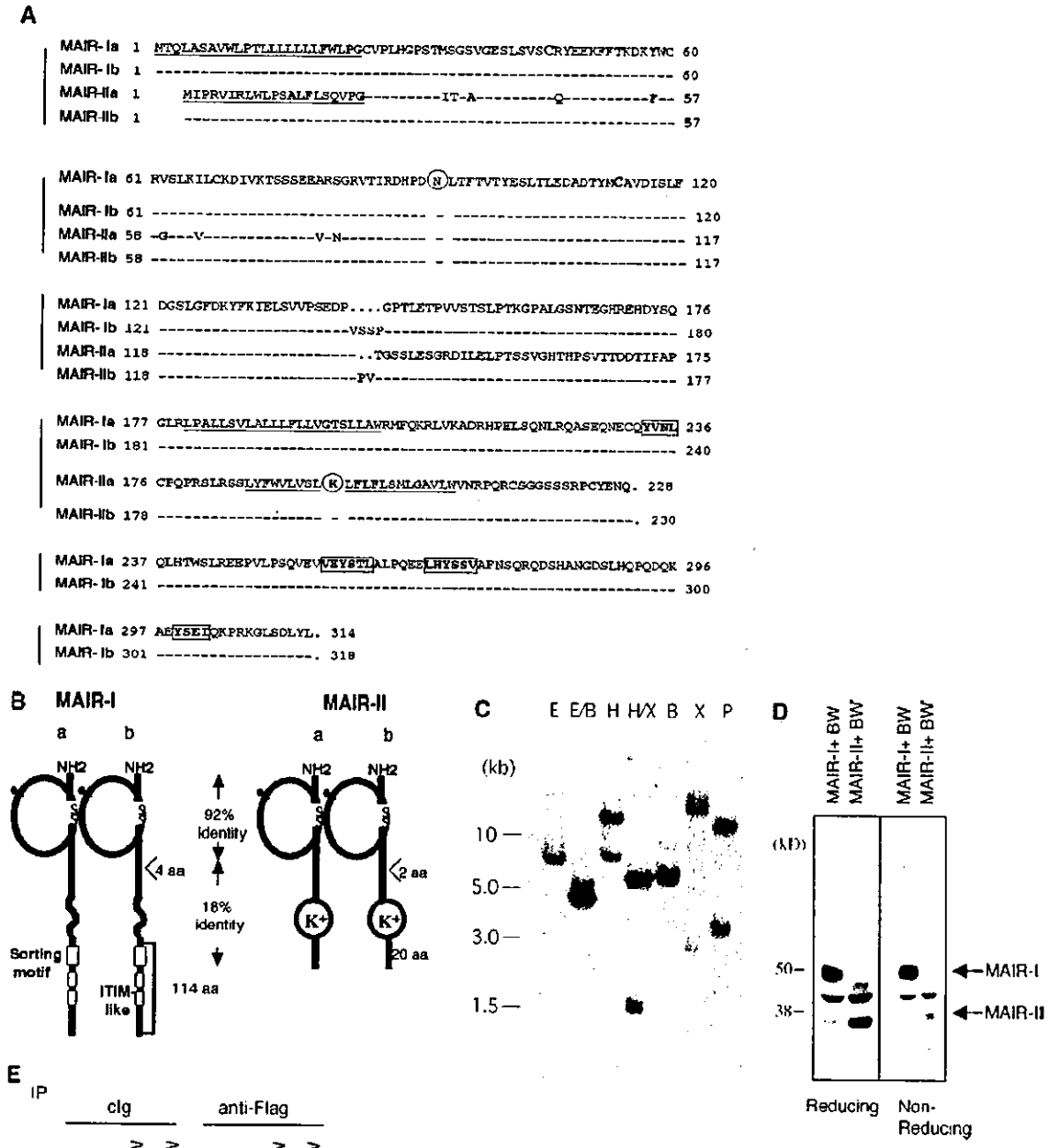

Figure 1. Molecular and biochemical characteristics of MAIR-I and MAIR-II. (A) Predicted aa sequences of MAIR-I and MAIR-II. The putative leader and transmembrane domain are underlined. Potential N-linked glycosylation sites in the extracellular domain and the charged aa residue in the transmembrane region are circled. Potential cysteine residues involved in disulfide bonding of the Ig-like domains are indicated in bold. ITIM-like or sorting motif in the cytoplasmic domain are boxed. The cDNA sequence data are available from GenBank/EMBL/DDBJ under accession nos. AB091765, AB091766, AB091767, and AB091768 (*MAIR-Ia*, *MAIR-Ib*, *MAIR-IIa*, and *MAIR-IIb*, respectively). (B) Schematic diagram of MAIR-I and MAIR-II proteins. A pair of cysteine residues in the extracellular portion potentially able to participate in intrachain disulfide bonding for the formation of Ig-like domains are indicated. (C) Southern blot analysis of genomic *MAIR-I* and *MAIR-II*. Mouse genomic DNA was digested with the indicated enzymes (E, EcoRI; B, BamHI; H, HindIII; X, XbaI; and P, PstI) and probed with the cDNA encoding the extracellular portion of MAIR-I. (D) BW5147 cells expressing the Flag-tagged MAIR-I or MAIR-II were lysed and proteins were analyzed by immunoblotting with anti-Flag mAb under reducing and nonreducing conditions. (E) BW5147 cells expressing the Flag-tagged MAIR-I or parental BW5147 cells were lysed and proteins were immunoprecipitated with anti-Flag. Precipitates were treated or not with *N*-glycosidase F and immunoblotted with anti-Flag mAb under nonreducing conditions.

DNA, using the cDNA encoding the conserved Ig-like domain in the extracellular domain of MAIR-I and MAIR-II, demonstrated a simple hybridization pattern, suggesting that each MAIR-I and MAIR-II is encoded by a single gene (Fig. 1 C). The *MAIR-I* and *MAIR-II* genes are located to the proximal region of the E2 band of mouse chromosome 11 and consist of six and four exons, respectively, as determined by FISH and a genomic DNA sequence database (unpublished data). Database search demonstrated that MAIR-I and MAIR-II are most similar to human CMRF-35-H9 (31) with 44% homology and to human CMRF-35 (31) with 49% homology, respectively. Moreover, both CMRF-35-H9 and CMRF-35 genes are located near to human chromosome 17, syntenic region of mouse chromosome 11 (32), suggesting that these are the human homologues to murine MAIR-I and MAIR-II.

Mouse T cell leukemia BW5147 cells were transfected with the *MAIR-Ia* and *MAIR-IIa* cDNAs tagged with Flag peptide at the NH_2 terminus, which resulted in surface expression of the receptor as detected by immunofluorescence using an anti-Flag mAb (unpublished data). Immunoprecipitation of the Flag-tagged MAIR-Ia and MAIR-IIa receptors on the BW5147 transfectants with an anti-Flag mAb revealed ~50 and ~35 kD proteins, respectively, when analyzed under both reducing and nonreducing conditions (Fig. 1 D). The mobility of MAIR-Ia decreased from ~50 to ~45 kD after treatment with *N*-glycosidase F, which is consistent with the size of the polypeptide predicted from the *MAIR-I* cDNA and the presence of one potential N-linked glycosylation site in the extracellular domain (Fig. 1 E).

Expression of MAIR-I and MAIR-II. Northern blot analysis using the full-length *MAIR-Ia* cDNA, containing the conserved cDNA sequence of the *MAIR-I* and *MAIR-II*, as a probe demonstrated that *MAIR-I* and/or *MAIR-II* transcripts were detected in lymphohematopoietic tissues, including spleen and bone marrow, but not in thymus and nonhematopoietic organs (Fig. 2 A). We also observed that peritoneal macrophages express significant amount of *MAIR* transcripts, which were up-regulated in these cells after in vivo stimulation with thioglycollate. The preferential expression of *MAIR* transcript was also observed in myeloid cell lines, including 416B, WEHI3, RAW, and M1 cells (Fig. 2 A).

To further analyze the expression of the MAIR-I and MAIR-II on hematopoietic cells, RNA was obtained from lymphohematopoietic progenitors and lineage-committed cells purified by flow cytometry from the bone marrow, thymus, and spleen. RT-PCR analysis using the specific primers for *MAIR-I* and *MAIR-II* demonstrated that both the transcripts were expressed in multilineage cells, including lymphohematopoietic progenitors, granulocytes, macrophages, erythroid cells, and B cells in bone marrow, and in T, B, and $NK1.1^+$ cells in the spleen. However, neither of the *MAIR-I* and *MAIR-II* transcripts was detected in immature and mature T cells in the thymus (Fig. 2 B).

To examine the cell surface expression of the MAIR-I and MAIR-II proteins, we generated monoclonal antibodies TX-8 and TX-13, which preferentially react to MAIR-I and MAIR-II, respectively (Fig. 3 A). Analysis of spleen and bone marrow cells by flow cytometry showed that MAIR-I is expressed on the majority of myeloid cells, including macrophages, dendritic cells, granulocytes, and bone marrow–derived cultured mast cells, and MAIR-I is expressed on a subset of B cells, but neither on T nor NK cells (Fig. 3, B and D). In contrast, MAIR-II protein is detected only on cell surface of subsets of B cells and peritoneal macrophages (Fig. 3, B and E). These results indicated that the transcript's expressions of MAIR-I and MAIR-II do not always result in cell surface expression of the proteins. To further characterize the B cell subsets expressing MAIR-I or MAIR-II, spleen cells were simultaneously stained with anti-CD21 and anti-CD23 mAbs in combination with either anti–MAIR-I or anti–MAIR-II. The marginal zone B cells that are characterized by cell surface phenotype of $CD21^{hi}CD23^{lo}$ express higher amount of MAIR-I and MAIR-II than the $CD21^{int}CD23^{hi}$ follicular B cells (Fig. 3 C; reference 33). These results suggest that marginal zone B cells consist of the major population of MAIR-II expressing B cell subset in spleen.

To examine regulatory mechanisms of the proteins expression on cell surface, purified B cells from spleen were cultured in medium in the presence or absence of LPS, resulting in a significant up-regulation of MAIR-II on the cell surface in both the culture condition (Fig. 3 F), although we did not observe any modulation of MAIR-I and MAIR-II proteins expressions on macrophages from spleen in the same culture condition (not depicted). Although no MAIR-I and MAIR-II proteins were detected on the NK cell surface despite the abundant presence of

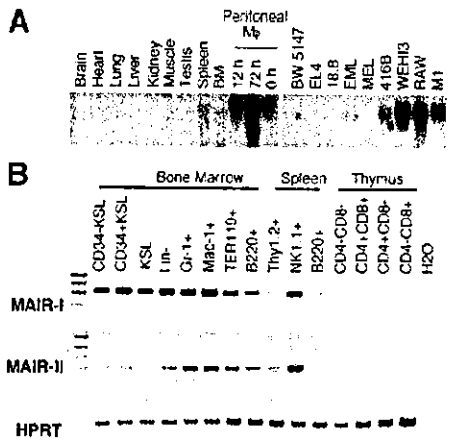

Figure 2. Expression of MAIR-I and MAIR-II transcripts. (A) Expression of MAIR-I and/or MAIR-II transcripts was analyzed by Northern blot analysis using cDNA encoding MAIR-I extracellular portion as a probe. The comparable amount of β-actin transcript expression in each lane using β-actin cDNA was confirmed (not depicted). (B) cDNA, adjusted to comparable quantities using a HPRT control, was prepared from purified cells by cell sorter, as indicated. These cDNA and water (used as a negative control) were used as templates for RT-PCR. PCR products were amplified using specific primers for MAIR-I and MAIR-II.

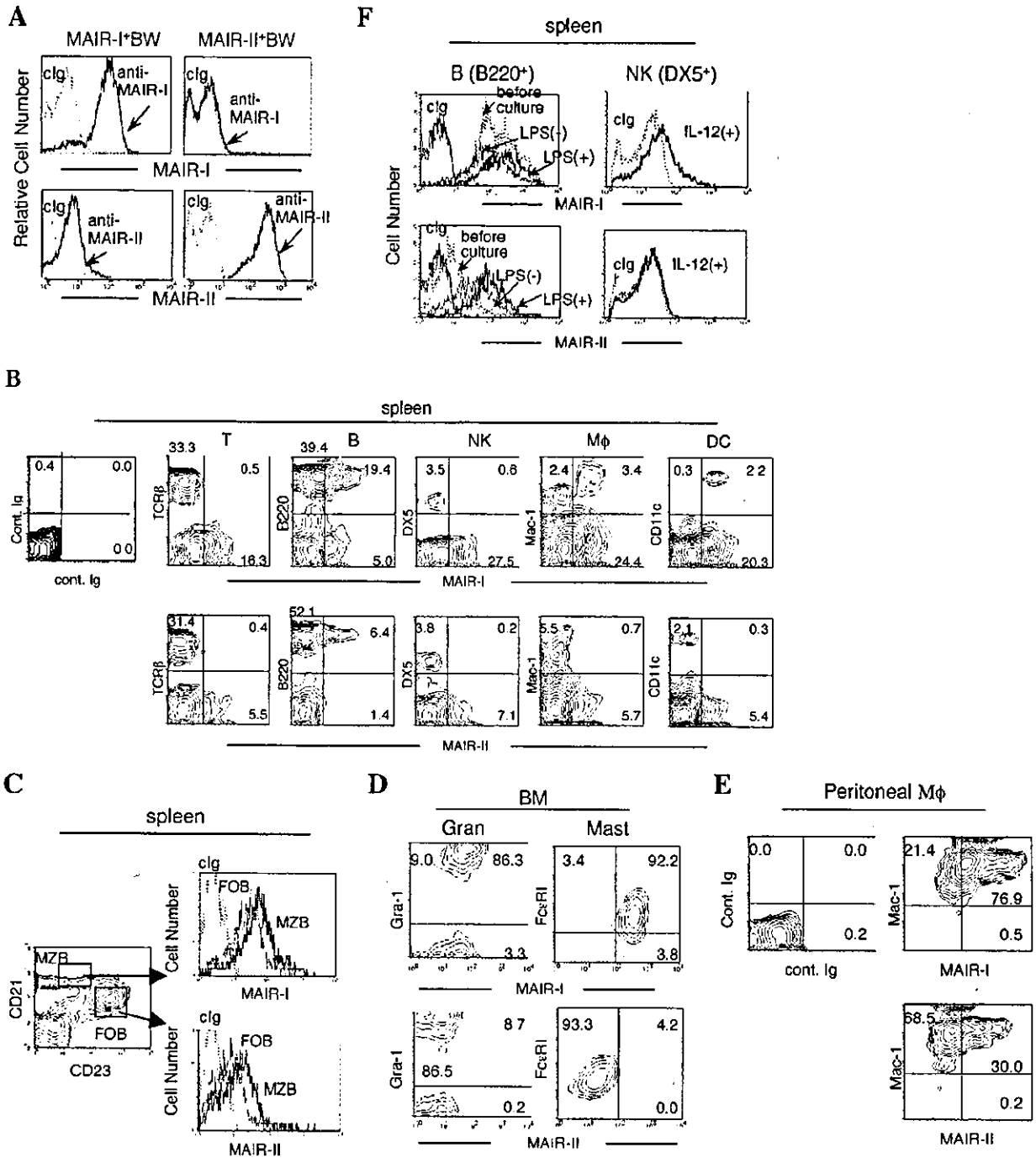

Figure 3. Cell surface expression of MAIR-I and MAIR-II proteins. (A) BW5147 transfectants expressing MAIR-I or MAIR-II were stained with control rat Ig or anti-MAIR-I (TX-8 mAb) or anti-MAIR-II (TX-13 mAb), followed by allophycocyanin-conjugated streptavidin. (B, D, and E) Spleen, bone marrow, or peritoneal macrophages from C57/BL6 mice were stained with either biotin-conjugated F(ab')2 fragments of anti-MAIR-I or anti-MAIR-II and the PE-conjugated mAbs indicated, followed by allophycocyanin-conjugated streptavidin. Greater than 99% of cells stained with F(ab')2 fragments of control Igs were present in the bottom left quadrant of the contour plots (B and D, and not depicted in C). (C) Spleen cells were stained with FITC-conjugated anti-CD21, PE-conjugated anti-CD23, and biotin-conjugated anti-MAIR-II monoclonal antibodies, followed by allophycocyanin-conjugated streptavidin. MAIR-I and MAIR-II expression on the $CD21^{lo}CD23^{lo}$ (marginal zone B cells [MZB]) and $CD21^{mo}CD23^{hi}$ (follicular B cells [FOB]) cells were analyzed by flow cytometry. (E) $B220^{+}$ B cells purified from splenocytes or total splenocytes were cultured for 48 h or not in the presence or absence of LPS or IL-12, as indicated, and stained with either biotin-conjugated F(ab')2 fragments of control Ig, anti-MAIR-I or anti-MAIR-II and the FITC-conjugated B220 or DX5 mAb, followed by allophycocyanin-conjugated streptavidin. Cells were gated according to B220 or DX5 expressions and analyzed by flow cytometry. Data are representative in several independent experiments.

their transcripts, IL-12 stimulated cell surface expression of MAIR-I, but not MAIR-II, on NK cells (Fig. 3 F).

MAIR-I Mediates Endocytosis. The cytoplasmic domain of the MAIR-I contains a possible tyrosine-based sorting motif (Fig. 1 A, YVNL), implicated in endosome and lysosome targeting of diverse proteins and involved in agonist-induced internalization (29, 30). To investigate whether the MAIR-I internalizes upon cross-linking, MAIR-I expressed on peritoneal macrophages were cross-linked with anti–MAIR-I mAb and incubated at 4 or 37°C for 1 h. Some of the cells were treated with trypsin to remove the cell surface MAIR-I that did not undergo internalization. Treatment with trypsin significantly decreased the fluorescence intensity of the cells, which were incubated at 4°C after cross-linking (Fig. 4 A). By contrast, the fluorescence remained constant in the cells, which were incubated at 37°C after cross-linking, despite treatment with trypsin. This suggests that cross-linking the MAIR-I induced the receptor internalization during culture at 37°C. To confirm MAIR-I internalization upon cross-linking, the Ba/F3 transfectants expressing the Flag-tagged MAIR-I at the NH_2 terminus were incubated with anti-Flag mAb, cross-linked with FITC-labeled secondary antibody, and incubated at 37°C for 30 min. Although green fluorescence was detected only at the cell surface before incubation, it was abundantly observed in the cytoplasm of the transfectants 30 min after incubation at 37°C under confocal scanning laser microscope (Fig. 4 B), indicating that MAIR-I underwent internalization after cross-linking. In contrast, we did not detect internalization of the MAIR-I mutated at the tyrosine residue 233 ($Y\text{-}F^{233}$) in the sorting motif (Fig. 4 B), indicating that the tyrosine at residue 233 is responsible for the MAIR-I internalization.

MAIR-I Recruits the Tyrosine Phosphatase SHIP. The existence of the ITIM-like sequences in the cytoplasmic region of MAIR-I suggested that MAIR-I is tyrosine phosphorylated and may recruit SH2-containing tyrosine phosphatases. Therefore, we first examined whether MAIR-I expressed on bone marrow–derived cultured mast cells were tyrosine phopshorylated by the stimulaion with pervanadate. As demonstrated in Fig. 5 A, stimulation with pervanadate significantly induced tyrosine phosphorylation of the MAIR-I (Fig. 5 A). Immunoprecipitation of the protein tyrosine phosphatases, SHP-1 and SHP-2, and SHIP demonstrated that MAIR-I associated with SHIP, but not SHP-1 and SHP-2, upon stimulation of mast cells with pervanadate (Fig. 5 B). These results suggest that MAIR-I may mediate inhibitory signal upon phosphorylation of the tyrosines in the cytoplasmic region.

MAIR-I Inhibits IgE-mediated Serotonin Release from Mast Cells. To address a functional role of MAIR-I in immune responses, mast cells were loaded with [^{3}H]serotonin and stimulated with an IgE mAb plus $F(ab')_2$ fragments of anti–MAIR-I mAb, followed by coligation with a common secondary reagent. As demonstrated in Fig. 5 C, cross-linking MAIR-I with anti–MAIR-I mAb inhibited IgE-mediated serotonin release from bone marrow–derived mast cells in

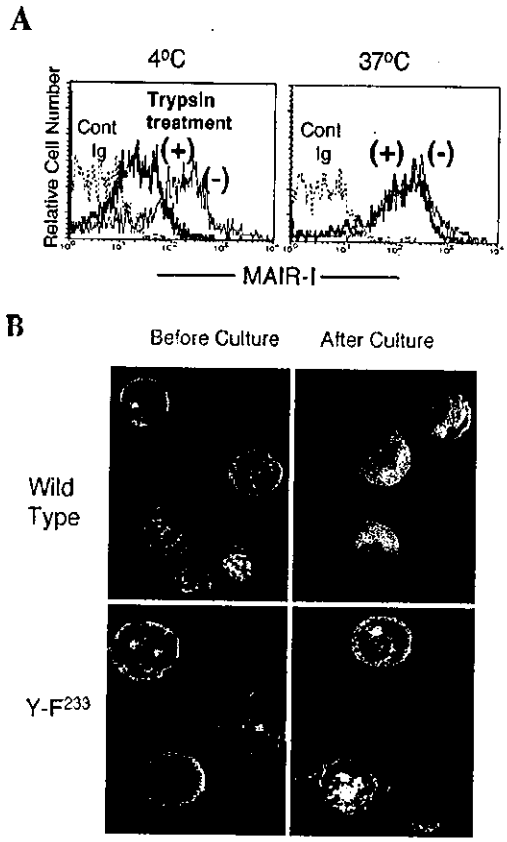

Figure 4. Internalization of MAIR-I. (A) Peritoneal macrophages were incubated with biotin-labeled anti–MAIR-I mAb (TX-8), followed by allophycocyanin-labeled streptavidin at 4 or 37°C for 30 min. The cells were treated (+) or not (−) with trypsin and analyzed by flow cytometry. (B) Ba/F3 transfectants expressing Flag-tagged wild-type and mutated MAIR-I were incubated with anti-Flag mAb, followed by cross-linking with FITC-labeled anti–mouse IgG secondary antibody at 4°C. Cells were incubated or not at 37°C for 30 min, fixed, mounted with VECTASHIELD including DAPI, and analyzed using a confocal scanning laser microscope. Data are representative in several independent experiments.

a dose-dependent manner. These results indicate that MAIR-I transduces an inhibitory signal, resulting in suppression of mast cell degranulation triggered by FcεRI-mediated activation signals.

MAIR-II Associates with DAP12. In contrast to MAIR-I, MAIR-II has a short cytoplasmic tail and a positively charged aa residue in the transmembrane domain. To test a noncovalent association of MAIR-II with an adaptor transmembrane protein, such as the FcεRIγ or DAP12, 293T cells, which express neither FcεRIγ nor DAP12, were transfected with *MAIR-II* cDNA and either *FcεRIγ* or *DAP12*. The transfectants were lysed in 1% digitonin buffer and immunoprecipitated with anti-FcεRIγ or anti-DAP12, and the isolated proteins were analyzed by immunoblotting with anti–MAIR-II. As demonstrated in Fig. 6 A, MAIR-II was coimmunoprecipitated with DAP12, but not with FcεRIγ, suggesting the physical association of MAIR-II with DAP12. Similary, MAIR-II

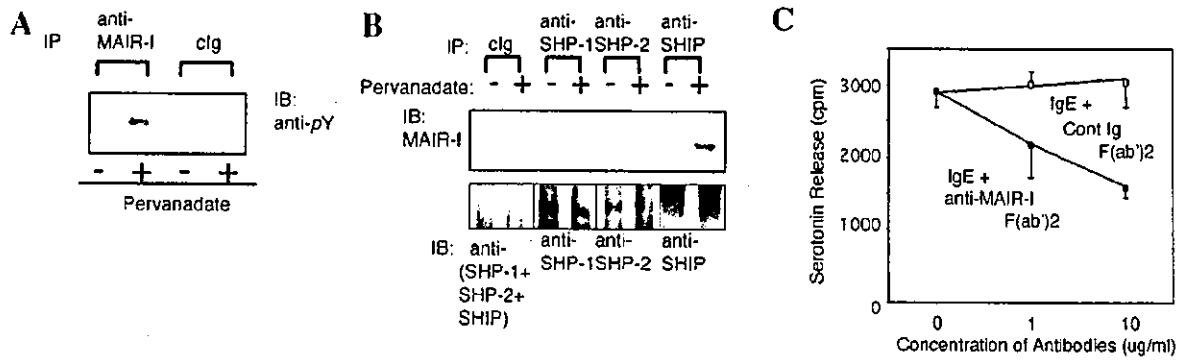

Figure 5. MAIR-I recruits the tyrosine phosphatase SHIP and inhibits serotonin release from mast cells. (A and B) Mast cells, derived from bone marrow cells after culture in the presence of IL-3 and stem cell factor (SCF), were stimulated or not with pervanadate for 10 min at 37°C and lysed in 1% NP-40 (A) or digitonin (B) buffer and immunoprecipitated with cIg, anti-MAIR-I, anti-SHP-I, anti-SHP-II, or anti-SHIP. The immunoprecipitates were immunoblotted with antiphosphotyrosine mAb (A) or anti-MAIR-I (B). (C) Mast cells were loaded with [^{3}H]serotonin and stimulated with an IgE mAb plus either F(ab')2 fragments of anti-MAIR-I or control rat IgG, followed by coligation with a common secondary reagent. [^{3}H]Serotonin release into the supernatants was measured by a liquid scintillation counter. Data are representative in several independent experiments.

was also coimmunoprecipitated with endogenous DAP12, but not FcεRIγ, in the lysates of mouse macrophage cells RAW after transfection with *MAIR-II* alone (Fig. 6 B). To confirm the physiological association of MAIR-II with DAP12 in primary cells, spleen cells were stimulated with LPS for 48 h, resulting in the up-regulation of MAIR-II expression of B cells and macrophages (unpublished data). The stimulated spleen cells were lysed in 1% digitonin buffer and immunoprecipitated with anti-FcεRIγ or anti-DAP12. Immunoblotting of the isolated proteins with anti-MAIR-II again demonstrated the coimmunoprecipitation of MAIR-II with the DAP-12, but not with the FcεRIγ (Fig. 6 C), indicating that DAP12 is the physiological partner for MAIR-II of stimulated B cells and/or macrophages in the spleen. These results were in agreement with the observation that DAP12 expression on cell surface of 293T cells depended on the expression of MAIR-II, although MAIR-II does not require DAP12 for cell surface expression (Fig. 6 D).

MAIR-II Stimulates Proinflamatory Cytokines and Chemokine Secretions from Macrophages. Because macrophages abundantly express DAP12 (34), we investigated a functional role of MAIR-II–mediated signaling in immune responses by macrophages. Macrophage cells, RAW, were transfected with Flag-tagged *MAIR-II* cDNA at the NH_2 terminus and stimulated with control Ig or anti-Flag. Cross-linking MAIR-II with anti-Flag significantly stimulated the production of TNF-α from the transfectants (Fig. 7). We further examined whether MAIR-II mediates TNF-α secretion from primary macrophages from peritoneal cavity. As shown in Fig. 7, TNF-α secretion from peritoneal macrophages was significantly increased upon cross-linking of MAIR-II. Similarly, engagement of MAIR-II stimulated IL-6 and MCP-1 secretions from peritoneal macrophages (Fig. 7). However, we did not observe a significant increase of IL-12 secretion from peritoneal macrophages after cross-linking MAIR-II (unpublished data). These results suggest that MAIR-II mediates activation signal in macrophages, leading to cytokine and chemokine secretion from macrophages.

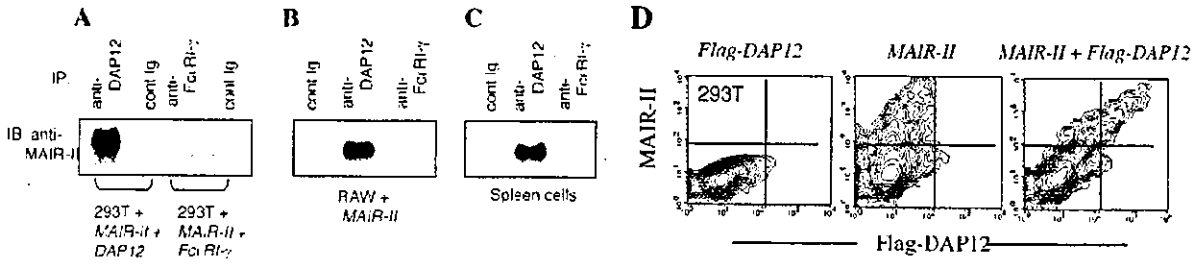

Figure 6. Physical association of MAIR-II with DAP12. (A–C) 293T and RAW cells, which were transfected with cDNA as indicated, and spleen cells after stimulation with LPS were lysed in digitonin buffer, immunoprecipitated with control Ig, anti-DAP12, or anti-FcεRIγ, and immunoblotted with anti-MAIR-II (TX-100). (D) 293T cells were transfected with *Flag-tagged DAP12*, *MAIR-II*, or a combination of *Flag-tagged DAP12* and *MAIR-II*, and stained with biotin-conjugated anti-MAIR-II and FITC-conjugated anti-Flag mAbs, followed by allophycocyanin-conjugated streptavidin. Cell surface expression of MAIR-II and DAP12 was analyzed by flow cytometry.